META-ADAPTIVE PROMPT DISTILLATION FOR FEW-SHOT VISUAL QUESTION ANSWERING

Anonymous authors
Paper under double-blind review

ABSTRACT

Large Multimodal Models (LMMs) often rely on in-context learning (ICL) to perform new visual question answering (VQA) tasks with minimal supervision. However, ICL performance, especially in smaller LMMs, does not always improve monotonically when increasing the number of examples. We hypothesize that this happens because the LMM is overwhelmed by extraneous information in the image embeddings that is irrelevant to the downstream task. To address this, we propose a meta-learning approach that induces few-shot capabilities in LMMs through a fixed set of soft prompts distilled from task-relevant visual features, which are adapted at test time using a small number of examples. We facilitate this distillation through an attention-mapper module that can be easily integrated with any LMM architecture and is jointly learned with soft prompts. Evaluation on the VL-ICL Bench shows that our method successfully achieves task adaptation in low-data regimes with just a few gradient steps, outperforming ICL by 21.2%. Comparisons with parameter-efficient finetuning methods demonstrate that meta-learning further enhances this adaptation by 7.7% for various VQA tasks.[1]

1 INTRODUCTION

Humans have the remarkable ability to quickly learn new tasks in multimodal environments with just a few trial-and-error attempts. Extensive research in cognitive science suggests that this ability arises from learning hierarchical abstractions and maintaining shared structural priors across related tasks based on past experiences (Griffiths et al., 2019; Finn, 2018; Kirsch & Schmidhuber, 2022). Drawing on this prior knowledge enables rapid learning in new situations and reduces the need for large amounts of task-specific demonstrations (Finn et al., 2017).

Large Multimodal Models (LMMs) are able to perform a multitude of tasks ranging from reasoning to fine-grained image understanding and visual question answering (Liu et al., 2024; Li et al., 2023a; Laurençon et al., 2024). They are typically built on top of a base Large Language Model (LLM) by supplementing it with a vision encoder and a connecting module that acts as a bridge for different modalities to interact. When (pre)trained at sufficient scale and finetuned on a wide range of multimodal tasks (with natural language instructions), LMMs can learn *new* tasks by virtue of in-context learning (ICL), i.e., by being prompted with a few input-output examples, without requiring any updates to model parameters (Zhao et al., 2024; Zong et al., 2025; Coda-Forno et al., 2023). Although the training-free nature of ICL has led to its rapid adoption across tasks and domains, its underlying mechanism remains ill-understood (Hendel et al., 2023; Huang et al., 2024) and its empirical behaviour can be inconsistent.

Zong et al. (2025) demonstrate that ICL is most effective for large-scale LMMs ($\sim$72B parameters), while smaller models ($\leq$7B parameters) struggle with increasing in-context examples and their performance either plateaus or deteriorates, even when extending the context length or giving detailed instructions. They attribute this limitation to the fact that smaller models struggle with the large number of image tokens in long sequences. They become confused and perform the task haphazardly or default to their parametric knowledge, effectively ignoring the in-context examples. Figure 1 shows a failure case from the Fast Open-Ended MiniImageNet dataset (Tsimpoukelli et al., 2021), using LLaVA-OneVision-7B (Li et al., 2025). The task is framed in a 2-way N-shot format where a *support*

[1]We provide our code for better reproducibility.

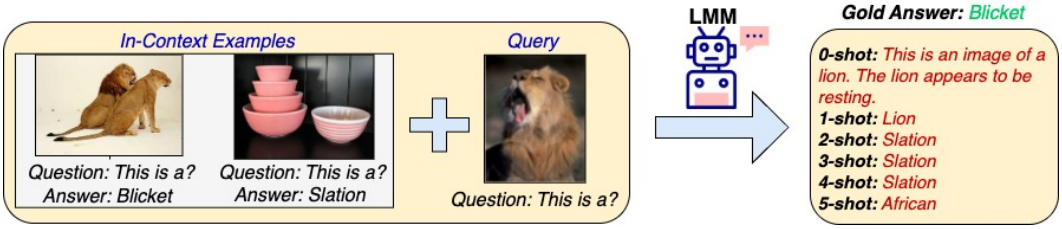

Figure 1: Failure case of LLaVA-OneVision-7B (Li et al., 2025) on an example from the Fast Open-Ended MiniImageNet classification task (Tsimpoukelli et al., 2021). When no in-context examples are provided (0-shot), the model generates a generic description of the image. As more examples (shots) are added, it begins to learn the answer format (single word), but still fails to grasp the task, producing incorrect or irrelevant predictions. We only show the in-context examples (left) for 2-way 1-shot setting for the sake of brevity but provide model predictions (in red) for up to 5 shots.

set with N labeled examples of two classes is provided. The model uses ICL with the support set to classify new *query* examples from the two classes. Without any support set or in-context examples (0-shot), the model outputs a generic description about the image based on parametric knowledge and ultimately fails to answer correctly, despite being prompted with a few examples.

Building on this observation, we hypothesize that effective few-shot adaptation at test time may be compromised by the information added by the image embeddings. While a set of more precise image embeddings would be preferable, their continuous nature makes it challenging to distill task-specific information from them. As an alternative, we propose to *learn* a fixed set of *new* embeddings that can be easily finetuned at test time. This idea of task adaptation has gained significant traction in the literature through *prompt tuning* (Lester et al., 2021) which finetunes a set of continuous *soft* prompts while keeping the underlying language model frozen; the prompts are prepended in the context at test time, effectively steering the model toward the desired task. Our approach learns new tasks using soft prompts that receive task information from the LLM in the form of loss gradients during finetuning. These gradients update the soft prompts which when fused with the image embeddings are able to distill relevant features from them. To facilitate this fusion, we propose an attention-mapper that uses a multi-head attention (Vaswani et al., 2017) architecture for extracting relevant task-specific image information and can be substituted in the projection layer of any LMM architecture.

Our approach relies on rapidly adapting to new tasks at test time using only a few examples, which is not addressed by traditional finetuning methods. Prior work (Finn et al., 2017; Ravi & Larochelle, 2017) addressed this challenge by training a meta-learner that can infer an optimal learning strategy for a new task after being exposed to a distribution of tasks. We apply this procedure to our multimodal prompt distillation setting by employing the widely known MAML algorithm (Finn et al., 2017) and use its lightweight first-order approximation to train the attention-mapper and soft prompts. We focus on visual question answering (VQA; Antol et al. 2015; see example in Figure 1), a general-purpose task often used to evaluate the image understanding capabilities of LMMs, and demonstrate the benefits of MAML training applied to LMM architectures. Our contributions are as follows:

- We introduce MAPD (**M**eta-**A**daptive **P**rompt **D**istillation), an alternative to in-context learning that meta-learns a fixed set of soft prompts within large multimodal models (LMMs) via distillation. MAPD enables adaptation to new tasks with a few examples using a few gradient updates at test time, and consistently improves performance as the number of shots increases. To our knowledge, this is the first exploration of meta-learned prompt distillation for cross-task generalization in LMMs under low-data settings.
- We propose a flexible attention-mapper module, inspired from Najdenkoska et al. (2023), which can be easily incorporated into the projection layer of any LMM architecture. It is trained jointly with *soft* prompts and can be easily adapted at test-time to facilitate the distillation of task-specific visual information.
- Extensive evaluation on VL-ICL Bench.[2] (Zong et al., 2025), a diverse benchmark for image perception and mathematical reasoning, demonstrates that our approach outperforms ICL and several other prompt distillation and parameter-efficient finetuning methods.

[2]We only focus on single-image few-shot VQA tasks and leave the multi-image scenario for future work.

2 Related Work

Our approach, Meta-Adaptive Prompt Distillation (MAPD), builds upon several existing research areas including few-shot learning, prompt tuning and test-time adaptation.

Multimodal Few-shot Learning Learning from a few examples has been a long-standing goal in machine learning. Early work by Vinyals et al. (2016) introduced Matching Networks for one-shot image-to-text classification. This approach leverages a support set of labeled images to classify an unlabeled query image, laying the foundation for few-shot learning in vision tasks. With the advent of large language models (LLMs) and large multimodal models (LMMs; Alayrac et al. 2022; Zhao et al. 2024), in-context learning (ICL; Zhao et al. 2024; Lester et al. 2021) has emerged as a popular method for few-shot adaptation. ICL involves providing a few input-output examples directly in the model's prompt without updating its parameters. While this is a computationally inexpensive method, its performance for LMMs can be inconsistent (Zong et al., 2025) and may even degrade as more examples are added, particularly in smaller models.

Test-Time Adaptation These methods aim to dynamically adapt models during inference on test examples, that may have distributional differences from the training data. This adaptation can either involve training of model parameters (Hardt & Sun, 2024) or can be entirely training free (Karmanov et al., 2024). Additionally, previous work (Hu et al., 2025) has taken advantage of parameter-efficient finetuning (PEFT) methods such as prompt tuning (Lester et al., 2021) and LoRA (Hu et al., 2022) to resolve catastrophic forgetting issues during test time training and achieve state-of-the-art performance. Shu et al. (2022) propose Test-time Prompt Tuning (TPT), a method that adapts vision-language models for zero-shot classification by tuning soft prompts on image augmentations. Previous work (Najdenkoska et al., 2023; Li et al., 2023b) has also explored meta-learning of soft prompts for small models and a limited range of vision-language tasks such as fast-concept binding.

We extend upon this idea to provide an alternative for few-shot adaptation in LMMs. Specifically, we design a meta-learning procedure, namely MAPD, to learn soft prompts that can distill task-relevant visual features from image embeddings and can be rapidly adapted at test time for a variety of new tasks using a few examples. We show that MAPD can be applied to any LMM architecture and achieves state-of-the-art performance on visual question answering tasks (Antol et al., 2015).

3 Problem Formulation

3.1 Few-shot Visual Question Answering

Visual Question Answering (VQA; Antol et al. 2015) is a key task for evaluating the ability of vision-language models to understand images by accurately responding to questions about various aspects of visual content. These questions can vary widely, ranging from descriptions of objects inside bounding boxes (Krishna et al., 2017) to solving high-school geometry problems (Gao et al., 2025), but are mostly grounded in the visual information present in the image.

In VQA, we typically have a dataset $\mathcal{D} = \{(X_v^i, X_q^i, X_a^i)\}_{i=1}^{|\mathcal{D}|}$ where $X_v \in \mathcal{I}$, $X_q \in \mathcal{Q}$ and $X_a \in \mathcal{A}$, and $\mathcal{I}$ is the set of all images, $\mathcal{Q}$ the set of all questions, and $\mathcal{A}$ the set of all answers. Our goal is to learn a function f_θ parametrized by θ, that maximizes the likelihood of the answer given the image and the question, $\prod_{i=1}^{|\mathcal{D}|} p_\theta(X_a^i | X_v^i, X_q^i)$. Following the standard train-test paradigm in deep learning, we evaluate whether f_θ generalizes well by dividing dataset D into $(D^{\text{train}}, D^{\text{test}})$ such that maximizing the above likelihood on D^{train} also maximizes the likelihood of answer on D^{test}. A common assumption is that the size of D^{train} is large enough so that function f_θ does not overfit on D^{train}. In the context of *few-shot* VQA, we treat the in-context examples (or shots) given to an LMM during ICL as D^{train}. Since the examples in D^{train} are limited (as few as 1-shot), it becomes harder to avoid overfitting while training and still perform well on D^{test}. We conceptualize this problem as one of learning about an underlying task represented by D^{train} and adopt meta-learning (Finn et al., 2017) which exploits the shared structure across a distribution of tasks to learn a prior over model parameters, thereby enabling stable transfer to new tasks with limited data. In the following, we describe how we enforce this prior over parameters through the curation of *meta-tasks* containing few-shots. A sketch of our model architecture and training procedure is shown in Figure 2.

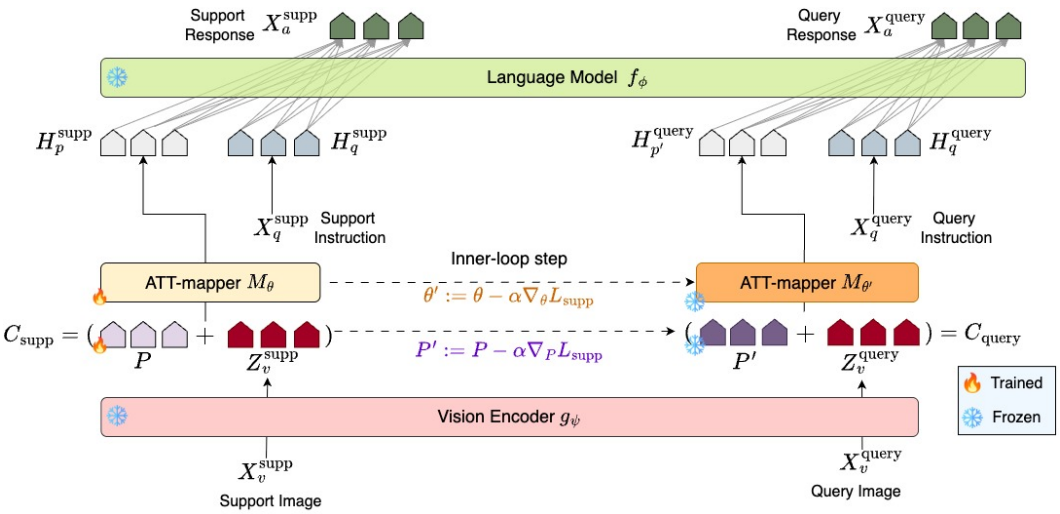

Figure 2: Our proposed MAPD framework based on LLaVA v1.5-7B (Liu et al., 2024): image embeddings are distilled into soft prompts P during instruction finetuning. The support set $(X_v^{\text{supp}}, X_q^{\text{supp}}, X_a^{\text{supp}})$ is processed initially to the obtain loss value L_{supp} which is used in the inner-loop to obtain task-specific parameters $\{\theta', P'\}$. Next, the query set $(X_v^{\text{query}}, X_q^{\text{query}}, X_a^{\text{query}})$ is used to calculate the query loss for the outer-loop meta-parameter optimization $\{\theta, P\}$.

3.2 Improving Task Understanding with Meta-tasks

The core idea of optimization-based meta-learning is to learn a good initialization of parameters, which when finetuned on a specific task, enables stable transfer for that task with a few gradient steps (Finn et al., 2017). To promote this capability, training involves processing batches of few-shot datasets that represent an underlying task. We refer to these few-shot datasets as *meta-tasks* and propose to create them from our finetuning data mixture based on the original LLaVA datasets. We provide details of our specific data mixture in Appendix A.1.1.

More formally, let $p(\mathcal{D})$ denote our data mixture. We create meta-task T^j by randomly sampling a fixed subset of examples from dataset $D^i \sim p(\mathcal{D})$ and partitioning the examples further into support and query sets $T^j = \{D^{\text{supp}}, D^{\text{query}}\}$. To be consistent with the notation introduced in Section 3.1, we treat the support set as $D^{\text{supp}} \equiv D^{\text{train}}$ and the query set as $D^{\text{query}} \equiv D^{\text{test}}$. We continue this process until all samples from D^i have been assigned to at least one meta-task. This meta-task construction is performed for *each dataset* in $p(\mathcal{D})$, resulting in meta-task distribution $p(\mathcal{T}^{\text{meta}})$. We now describe our model architecture designed to process these meta-tasks.

3.3 Model Architecture

We design our LMM architecture (Figure 2) based on the visual instruction tuning framework of LLaVA v1.5[3] (Liu et al., 2024) and further describe our modifications for incorporating the attention-mapper. For clarity, we omit the distinction between support and query sets in this section as both are processed in the same manner. As shown in Figure 2, the model consists of a pretrained CLIP ViT-L/14 visual encoder (g_ψ) with an aspect ratio of 336px; for an input image X_v, the encoder gives us hidden visual features Z_v which are then passed to the projection layer that consists of an attention-mapper M_θ responsible for extracting useful features from Z_v.

Attention Mapper We re-design the projection layer of LLaVA v1.5 to include soft prompts P by introducing an attention-mapper M_θ for improved *task-specific* feature extraction. Specifically, we prepend Z_v with a set of m learnable prompt tokens P to obtain a sequence $C = (P, Z_v)$ which is then passed to the attention-mapper (see Figure 2). Both prompt tokens P and weights θ are

[3]We adopt LLaVA v1.5 due to its simplicity and publicly available training code and datasets (Section A.1.1). This prevents mixing between training and test datasets and enables evaluation over unseen tasks. We demonstrate in Section 4.3 that our method can be easily applied to other LMM architectures.

initialized with Xavier Uniform initialization (Glorot & Bengio, 2010). We define the mapper as:

$$H_{p+v} = M_\theta(Q, K, V) = \sigma(QK^T) * V \tag{1}$$

where the query is $Q = M_\theta^q \cdot C$; , the key is $K = M_\theta^k \cdot C$; , the value is $V = M_\theta^v \cdot C$, and their corresponding matrices are $\{M_\theta^q, M_\theta^k, M_\theta^v\}$. The mapper computes the dot product of the query and key vectors which are then passed to a softmax function to compute activation scores for every feature in vector V. Finally, we extract the first m embeddings corresponding to the learnable prompt tokens from the set H_{p+v} that correspond to the task-specific image embeddings H_p. These are now passed to the LLM (f_ϕ) as prompts for further processing. We denote the trainable parameters for the attention-mapper with $\theta_p = \{\theta, P\}$.

Language Model The quality of the learned prompts highly depends on the underlying language model. We update the LLM of LLaVA v1.5 with the state-of-the-art Qwen2.5-7B-Instruct LLM, which has demonstrated strong performance on complex tasks such as mathematical reasoning and coding and supports the generation of up to 8K tokens. The LLM (f_ϕ) receives the concatenated sequence of image and text tokens to generate the answer $X_a = f_\phi([H_p, H_q])$. In this pipeline, only the attention mapper parameters θ_p are trained, making our approach parameter-efficient for cross-task generalization. The number of trainable parameters is approximately 24M (see Appendix A.1.2 for hyperparameters). The training objective maximizes the likelihood function, $p_{\theta_p}(X_a|X_v, X_q)$, parametrized by θ_p, where X_a is the answer, X_v is the image, and X_q is the question. For clarity, we refer to this model, namely LLaVA-ATT-Qwen2.5 7B, as our base LMM in the following sections.

3.4 Model Training

We train the attention mapper parameters to learn image-conditioned soft prompts in two stages following a curriculum learning procedure similar to LLaVA v1.5 (Liu et al., 2023). In the first-stage, which is aimed at feature alignment, the attention-mapper is pretrained on the LCS-558K subset of the LAION/CC/SBU dataset filtered with a more balanced concept coverage (Liu et al., 2023). Further details on pretraining are mentioned in Appendix A.1.3. In the second stage, which aims to distill task-specific image features into prompts H_p, the attention-mapper parameters θ_p are finetuned on diverse task-specific instructions. We describe our MAML-based finetuning procedure below and also introduce alternative methods which we compare against in our experiments.

3.4.1 Learning to Distill Prompts with First-order Meta Learning

Our prompt distillation procedure, MAPD, uses the model-agnostic first-order approximation of MAML (Finn et al., 2017) which aims to learn a robust initialization of meta-parameters that enable efficient adaptation to new tasks with just a few gradient updates. We borrow the implementation of Antoniou et al. (2019) and use their first-order version and (learnable) per-step learning rates (α) to further optimize the training process. We sample a batch B of meta-tasks from $p(\mathcal{T}^{\text{meta}})$ and use the support set of each task to convert θ_p into task specific parameters θ'_p with a few gradient steps. Equations (2) and (3) show a *single* step of this inner loop:

$$L_{\theta_p}^{\text{supp}} = \frac{-1}{|D^{\text{supp}}|} \sum_{i=1}^{|D^{\text{supp}}|} \log(p_{\theta_p}(X_a^i|X_v^i, X_q^i)) \tag{2}$$

$$\theta'_p = \theta_p - \alpha \nabla_{\theta_p} L_{\theta_p}^{\text{supp}} \tag{3}$$

The *outer* loop involves optimizing the meta-parameters which in our case are the original attention-mapper parameters θ_p on the query set using the task-specific parameters θ'_p:

$$L_{\theta'_p}^{\text{query}} = \frac{-1}{|D^{\text{query}}|} \sum_{i=1}^{|D^{\text{query}}|} \log(p_{\theta'_p}(X_a^i|X_v^i, X_q^i)) \tag{4}$$

$$\theta_p := \theta_p - \beta \sum_{j=1}^{|B|} \nabla_{\theta'_{p,j}} L_{\theta'_{p,j}}^{\text{query}} \tag{5}$$

Equation (5) is the first-order approximation of the meta-update in MAML (Finn et al., 2017) that treats the gradient of $\theta'_{p,j}$ w.r.t. θ_p for a meta task as a constant. This approximation avoids backpropagating through the entire computation graph of the inner loop and avoids the Hessian-vector product estimation of the query loss. This saves huge GPU memory while still approximating a gradient in the same direction as the true MAML gradient (Weng, 2018). We provide a sketch of MAPD training in Figure 2 and a more detailed algorithm in Appendix A.1.4 as Algorithm 1

3.4.2 Alternative Methods for Prompt Distillation

We also implement other prompt distillation methods based on our model architecture to compare their performance with MAPD on few-shot VQA tasks. We provide a more formal description of these methods below, highlighting important differences from our framework.

Multi-Task Prompt Distillation We define a multi-task baseline where we eliminate the bi-level optimization of MAPD. Specifically, at each iteration, we sample a batch of meta-tasks from $p(\mathcal{T}^{\text{meta}})$ and optimize the following loss per task:

$$L_{\theta_p} = \frac{-1}{N} \sum_{i=1}^{N} \log(p_{\theta_p}(X_a^i | X_v^i, X_q^i)) \tag{6}$$

such that $N = |D^{\text{supp}}| + |D^{\text{query}}|$. This loss is accumulated across the entire batch of meta-tasks used to update θ_p. We refer to this baseline as Multi-Task$^{\text{PD}}$.

In-Context Prompt Distillation Previous work (Chen et al., 2022; Min et al., 2022) suggests it is possible to meta-learn task information by reducing the bi-level optimization of MAML to a sequence prediction problem over in-context examples with the help of pretrained LLMs. We develop a method called In-Context$^{\text{PD}}$, where we concatenate the support set with each query example in a meta-task, and optimize the following loss function to distill this task information from LLMs into soft prompts:

$$L_{\theta_p} = \frac{-1}{|D^{\text{query}}|} \sum_{i=1}^{|D^{\text{query}}|} \log(p_{\theta_p}(X_a^i | X_v^i, X_q^i, D^{\text{supp}})) \tag{7}$$

Methods without Meta-tasks To further understand the benefit of curating meta-tasks (see Section 3.2), we compare with the original finetuning procedure of LLaVA-v1.5 7B but only train θ_p without any meta-tasks for fair comparison. We refer to this method as NoMeta-task$^{\text{PD}}$ in subsequent sections. We also compare with model averaging, which is computationally efficient and has been shown to increase performance on out-of-distribution datasets (Choshen et al., 2022; Wortsman et al., 2022).We separately finetune the attention-mapper on each dataset $D^i \sim p(\mathcal{D})$, and take an average of all dataset-specific parameters θ_p^i weighted by their corresponding dataset size ratios:

$$\theta_p^{\text{avg}} = \sum_{i=1}^{|\mathcal{D}|} \theta_p^i \cdot w^i \tag{8}$$

where $w^i = |D^i| \,/\, |\mathcal{D}|$. We refer to this baseline as Model-Avg$^{\text{PD}}$ in subsequent sections.

3.5 Test-Time Adaptation

After learning optimal parameters with MAPD and alternative distillation strategies, we adapt the attention-mapper to a new (test) task by finetuning for K gradient steps. We experiment with a range of K values and explain how we select the best one for a task in Appendix A.2.2. Given K steps, we finetune the parameters θ_p on the support set $D_{\text{test}}^{\text{supp}}$ of test task T_{test}^j and evaluate model performance on the query set $D_{\text{test}}^{\text{query}}$ for the same task.

4 Experimental Results

4.1 Evaluation Datasets

For evaluation purposes, our test datasets follow the same structure as the meta-tasks introduced in Section 3.2, with support and query examples. We use the recently introduced VL-ICL benchmark (Zong et al., 2025), designed to test the ICL capabilities of LMMs on various tasks like fast concept binding, multimodal reasoning, and fine-grained perception. Meta-tasks for testing are created by randomly sampling a support set from the training split of the VL-ICL datasets and a test/query set from their respective testing splits.[4] In line with our training pipeline, which exclusively utilizes

[4]We also keep a separate validation set for each VL-ICL dataset (sampled from the training split) to select the best model which we then evaluate on the test (query) set. More details can be found in Section A.2.2

Methods	MT	Open-MI	OP_IND	CLEVR	TextOCR
TTA with ICL					
NoMeta-task^{PD}	✗	43.8	12.1	18.0	6.8
Model-Avg^{PD}	✗	26.6	9.2	7.6	2.8
In-Context^{PD}	✓	51.1	20.6	24.1	23.8
Multi-Task^{PD}	✓	48.6	10.0	12.5	6.9
MAPD	✓	53.3	9.60	12.3	7.30
TTA with FT $\leq$ 30					
NoMeta-task^{PD}	✗	68.0	38.8	25.8	22.5
Model-Avg^{PD}	✗	63.1	40.0	29.1	21.5
In-Context^{PD}	✓	64.5	30.9	30.9	18.9
Multi-Task^{PD}	✓	74.6	45.1	29.9	22.9
MAPD	✓	**77.9**	**47.7**	**31.4**	**26.4**

Table 1: Evaluation on tasks from the VL-ICL Bench (Zong et al., 2025) with LLaVA-ATT-Qwen2.5 7B as the base LMM. Each method trains 24M attention-mapper parameters. We report the mean accuracy across shots $\{1, 2, 4, 5, 8\}$ and compare different prompt distillation approaches. TTA:Test-Time Adaptation, FT: Finetuning with $K \leq 30$ gradient steps, ICL: In-Context Learning, MT: Meta-Tasks used (✓) or not (✗) during training. More qualitative results can be found in Appendix A.2.5 and A.2.8.

LoRA	Open-MI	OP_IND	CLEVR	TextOCR
TTA with FT $\leq$ 30				
All LLM layers	55.1	13.3	15.1	10.4
[0-15] LLM layers	67.3	25.5	**30.0**	23.8
[0-15] LLM layers + ATT	**69.1**	**30.5**	28.7	**24.5**

Table 2: LoRA configurations applied to the base LMM and evaluated on the VL-ICL bench. ATT: Attention-Mapper; TTA: Test-Time Adaptation; FT: Finetuning with $K \leq 30$ gradient steps.

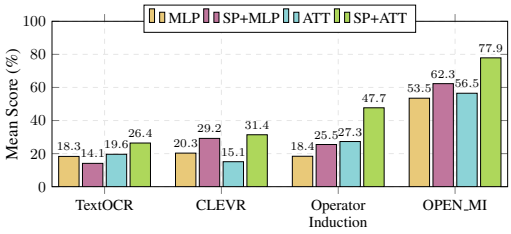

Figure 3: Comparison between different architectures for the projection layer in the base LMM. SP: Soft Prompts, ATT: Attention-Mapper, MLP: 2-layer MLP as originally used in LLaVA v1.5.

datasets containing a single image per example (see Section A.1.1), we focus solely on single image-to-text scenarios, leaving multi-image cases for future work. We report results on four tasks from VL-ICL: a) *Fast Open MiniImageNet (Open-MI)*, where the model must name new objects based on a few examples; b) *Operator Induction*, where the model must solve image tasks of the type $2 \; ? \; 7 =?$ given training examples like $1 \; ? \; 3 = 4$; c) *CLEVR Count Induction*, where the model must count objects that satisfy given attributes like "*shape: sphere*"; and d) *TextOCR*, where the model must transcribe highlighted text contained in an image. We provide more details on these tasks in Appendix A.2.1. The final model performance is calculated as the average across all meta-tasks.

4.2 Model Comparisons

Our results are summarized in Table 1, which compares MAPD against alternative prompt distillation methods (see Section 3.4.2) and reports the mean accuracy of up to eight shots. We compare two types of test-time adaptation methods, namely in-context learning (ICL) which prompts the underlying LLM with no distillation of image embeddings and finetuning (FT) with K $\leq$ 30 gradient steps, which are further distinguished based on whether they use meta-tasks during training. Results for individual shots are in Appendix A.2.3; additional results for more shots are in Appendix A.2.9[5].

Prompt distillation improves task induction in LMMs at test-time. Our results in Table 1 show that FT adaptation with few-shots (support examples) largely outperforms ICL at test time evaluated over query examples, with an average increase of 21.2% over all datasets. These results highly support our hypothesis that distilling task-specific information from image embeddings to create targeted prompts improves the few-shot capabilities of the underlying LLM (in our case Qwen-2.5-7B-Instruct). Additionally, our results show that finetuning just the attention-mapper parameters only requires a few gradient steps ($K \leq 30$) at test-time to generalize to unseen tasks and does not lead to overfitting over the support examples (Appendix A.2.2). For a one-to-one comparison, we look into In-context^{PD}, which performs better with FT on 3 out of 4 tasks compared to its ICL adaptation and enables prompting the underlying LLM with a fixed set of learned task-specific embeddings.

Meta-learning and meta-tasks improve few-shot learning. Table 1 shows that methods using meta-tasks are indeed superior. For ICL-based adaptation, In-Context^{PD} performs best, while for FT-based adaptation, our proposed approach, MAPD, achieves the best overall performance across all four datasets at test time. This further suggests that first-order MAML learns the best initialization of attention-mapper parameters θ_p. These parameters are subsequently adapted for a test task with a few gradient steps and few-shot examples to produce a precise set of soft prompts that improves

[5]We also provide ICL performance of publicly available models in Appendix A.2.4 for reference.

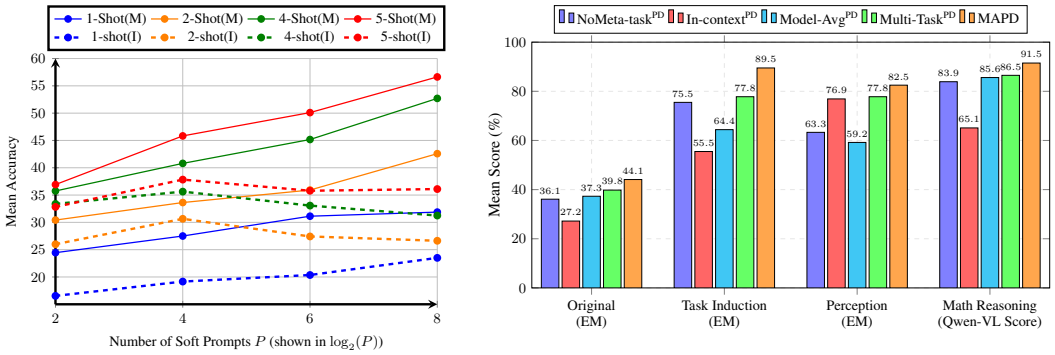

Figure 4: (a) **Left**: Performance comparison between MAPD+FT (M) and In-Context^{PD}+ICL (I). Mean Accuracy is computed across all VL-ICL datasets. We consider different prompt token lengths $P = \{4, 16, 64, 256\}$ which are shown in $\log_2(P)$ scale for different shots. (b) **Right**: Performance of different prompt distillation methods on three Operator Induction subtasks: Task Induction, Perception, and Math Reasoning. We report mean exact-match (EM; %) for 1,2 and 8-shots as defined in the VL-ICL Bench (Zong et al., 2025) except for Mathematical Reasoning, which uses mean ratings generated by Qwen-2.5-VL-32B-Instruct. More details can be found in Appendix A.2.8

LMM predictions on that task. Our detailed results in Table 7 in Appendix A.2.3 further show that for FT-based adaptation, MAPD is most effective in the 2-shot case for Operator Induction, surpassing Multi-Task^{PD} by 10%. Finally, MAPD with FT is the only approach that exhibits strictly monotonic improvements as the number of shots increases, showing better scaling behavior.

MAPD surpasses other efficient finetuning approaches for few-shot adaptation. We compare MAPD with LoRA (Hu et al., 2022), a state-of-the-art parameter-efficient finetuning (PEFT) approach. In Table 2, we integrate LoRA in the base LMM in three configurations and evaluate on VL-ICL: (1) naively applying LoRA to all underlying LLM layers (as done in LLaVA v1.5; Liu et al. 2023) increases the number of trainable parameters ($\sim$ 300M) and the model finds it difficult to converge within 30 gradient steps at test-time; (2) restricting LoRA to the first 16 LLM layers ($\sim$ 24M parameters) offers better test-time performance; and (3) adding LoRA to the attention-mapper layers further boosts performance as it provides some distillation over the image embeddings before prompting the underlying LLM. Ultimately, MAPD still outperforms the best LoRA configuration by an average of 7.7% across all VL-ICL datasets. This demonstrates that MAPD is the best choice for achieving fast test-time adaptation in low-data scenarios. We provide additional LoRA training details in Appendix A.1.3 and further detailed results can be found in Appendix A.2.3.

4.3 Ablation Studies and Analysis

In this section, we present ablation studies across various model architectures and sizes, along with a more in-depth analysis of the benefits of test-time fine-tuning using MAPD. Please refer to appendix for further ablations on testing 1) robustness to image perturbations (Appendix A.2.6) and 2) different few-shot selection strategies (Appendix A.2.7).

What are the benefits of the attention mapper and soft prompts? In Figure 3, we compare different architectural designs for the projection layer in the base LMM for rapid few-shot learning. We clearly see that MAPD benefits most by incorporating the attention-mapper and soft prompts (SP+ATT). We draw two key conclusions from this experiment: (1) distilling task-relevant information from CLIP embeddings with soft prompts yields substantial improvements, with an average gain of 16.3% across architectures. (2) replacing the 2-layer MLP used in LLaVA v1.5 with an attention mapper leads to an additional average gain of 13.1%, thanks to its inherent weighting mechanism of pairwise similarities over CLIP embeddings.

How does the number of soft prompts affect performance? We examine how MAPD's performance changes with the number of soft prompts across varying shot settings for VL-ICL datasets in Figure 4(a). Additionally, we show results of our best ICL approach, In-Context^{PD}, as a baseline for this comparison. We see that MAPD scales favorably and learns more consistent task information from

Vision Encoder	LLM	TTA	NoMeta-task^{PD}	Model-Avg^{PD}	In-Context^{PD}	Multi-Task^{PD}	MAPD
CLIP ViT-L/14	Qwen2.5-7B Instruct	ICL	43.8	26.6	51.1	48.6	**53.3**
		FT$\leq$30	68.0	63.1	64.5	74.6	**77.9**
CLIP ViT-L/14	Qwen2.5-3B Instruct	ICL	24.3	30.5	**48.3**	39.1	32.9
		FT$\leq$30	56.5	66.0	47.5	61.1	**67.3**
CLIP ViT-L/14	Vicuna v1.5-7B	ICL	20.0	26.2	46.3	29.1	**49.9**
		FT$\leq$30	69.1	74.9	66.7	70.3	**75.8**
SigLIP-SO400M	Qwen2.5-7B Instruct	ICL	42.6	40.7	47.3	**50.0**	43.6
		FT$\leq$30	52.0	56.5	56.0	59.3	**60.5**

Table 3: Comparison of various prompt distillation approaches under different LMM settings while keeping the attention-mapper and soft prompts fixed. We report mean accuracy across 1 to 5 shots for the Fast Open-Ended MiniImageNet benchmark. The original LLaVA-ATT-Qwen2.5 7B architecture is highlighted in gray. FT: Finetuning with K $\leq$ 30 gradient steps, ICL: In-Context Learning, TTA: Test-Time Adaptation. NoMeta-task^{PD} and Model-Avg^{PD} do not use meta-tasks.

gradient updates at test time as the number of soft prompts is increased. Furthermore, its marginal improvement per added prompt token is substantially greater when more shots are provided. In contrast, the performance of In-Context^{PD} generally deteriorates with more prompts and struggles to jointly attend to more examples and longer prompts.

To what extent does MAPD facilitate task understanding at test time? We take a closer look at how effectively MAPD captures task understanding at test time, using the Operator Induction task (See Figure 6) as a case study. To solve this task, the model should correctly (a) identify the operands in the query example (*Perception*); (b) identify the operation from few-shot examples (*Task Induction*); and (c) use its own mathematical knowledge over the identified elements to reason towards the answer (*Mathematical Reasoning*). To test whether the model understands these subtasks, we design specific prompts and modify query examples as listed in Appendix A.2.8. In Figure 4(b), we observe that MAPD outperforms other prompt distillation approaches on all three subtasks, leading to better performance on the original task. MAPD shows a major improvement for task induction with an increase of 11.7% compared to MultiTask^{PD}. We also observe that solving each subtask individually is easier than tackling the original task, as the latter requires integrating knowledge from all subtasks, which is challenging when only a few shots are available at test time. Finally, MAPD excels at mathematical reasoning, effectively utilizing the underlying LLM's reasoning capabilities.

Does MAPD generalize across different LMM architectures? We next examine different LMM architectures that affect MAPD's performance. Specifically, we report results in three settings that vary the underlying LLM and vision encoder: a) using a smaller LLM (Qwen2.5-3B-Instruct); b) using a different and relatively weaker LLM (Vicuna v1.5-7B); and c) using a different vision encoder, SigLIP (Zhai et al., 2023) . In Table 3, MAPD outperforms other baselines with FT adaptation across different model configurations on the Open_MI task, demonstrating its robustness and generalizability. Fine-tuning based test-time adaptation for prompt distillation substantially outperforms ICL, with average improvements of +24.6, +37.06, and +12.02 across the three settings, respectively. This highlights the significant benefits of test-time prompt distillation.

5 Conclusion

This work introduced Meta-Adaptive Prompt Distillation (MAPD), a novel meta-learning approach that endows LMMs with few-shot capabilities. MAPD employs a fixed set of soft prompts, distilled from task-relevant image features, which can be efficiently adapted at test time using only a few examples. A key component of our method is an attention-mapper module, which can be flexibly integrated with any LMM architectures and is jointly learned with soft prompts to facilitate distillation. Extensive evaluation on the VL-ICL benchmark shows that MAPD consistently outperforms traditional ICL and other efficient finetuning approaches across a diverse range of VQA tasks. Additional analysis (presented in Appendix A.3) suggests that MAPD with finetuning-based adaptation scales better as test-time computational budget is increased and is more data-efficient compared to ICL. Future work could focus on improving MAPD's computational efficiency for resource-constrained scenarios and extending it to multi-image tasks and complex reasoning problems.

REFERENCES

Jean-Baptiste Alayrac, Jeff Donahue, Pauline Luc, Antoine Miech, Iain Barr, Yana Hasson, Karel Lenc, Arthur Mensch, Katherine Millican, Malcolm Reynolds, Roman Ring, Eliza Rutherford, Serkan Cabi, Tengda Han, Zhitao Gong, Sina Samangooei, Marianne Monteiro, Jacob Menick, Sebastian Borgeaud, Andrew Brock, Aida Nematzadeh, Sahand Sharifzadeh, Mikolaj Binkowski, Ricardo Barreira, Oriol Vinyals, Andrew Zisserman, and Karen Simonyan. Flamingo: a visual language model for few-shot learning. In Alice H. Oh, Alekh Agarwal, Danielle Belgrave, and Kyunghyun Cho (eds.), *Advances in Neural Information Processing Systems*, 2022. URL https://openreview.net/forum?id=EbMuimAbPbs.

Stanislaw Antol, Aishwarya Agrawal, Jiasen Lu, Margaret Mitchell, Dhruv Batra, C Lawrence Zitnick, and Devi Parikh. Vqa: Visual question answering. In *Proceedings of the IEEE international conference on computer vision*, pp. 2425–2433, 2015.

Antreas Antoniou, Harrison Edwards, and Amos Storkey. How to train your MAML. In *International Conference on Learning Representations*, 2019. URL https://openreview.net/forum?id=HJGven05Y7.

Yanda Chen, Ruiqi Zhong, Sheng Zha, George Karypis, and He He. Meta-learning via language model in-context tuning. In Smaranda Muresan, Preslav Nakov, and Aline Villavicencio (eds.), *Proceedings of the 60th Annual Meeting of the Association for Computational Linguistics (Volume 1: Long Papers)*, pp. 719–730, Dublin, Ireland, May 2022. Association for Computational Linguistics. doi: 10.18653/v1/2022.acl-long.53. URL https://aclanthology.org/2022.acl-long.53/.

Leshem Choshen, Elad Venezian, Noam Slonim, and Yoav Katz. Fusing finetuned models for better pretraining, 2022. URL https://arxiv.org/abs/2204.03044.

Julian Coda-Forno, Marcel Binz, Zeynep Akata, Matthew Botvinick, Jane X Wang, and Eric Schulz. Meta-in-context learning in large language models. In *Thirty-seventh Conference on Neural Information Processing Systems*, 2023. URL https://openreview.net/forum?id=sx0xpaO0za.

Chelsea Finn, Pieter Abbeel, and Sergey Levine. Model-agnostic meta-learning for fast adaptation of deep networks. In *International conference on machine learning*, pp. 1126–1135. PMLR, 2017.

Chelsea B Finn. *Learning to learn with gradients*. University of California, Berkeley, 2018.

Jiahui Gao, Renjie Pi, Jipeng Zhang, Jiacheng Ye, Wanjun Zhong, Yufei Wang, Lanqing HONG, Jianhua Han, Hang Xu, Zhenguo Li, and Lingpeng Kong. G-LLaVA: Solving geometric problem with multi-modal large language model. In *The Thirteenth International Conference on Learning Representations*, 2025. URL https://openreview.net/forum?id=px1674Wp3C.

Xavier Glorot and Yoshua Bengio. Understanding the difficulty of training deep feedforward neural networks. In *Proceedings of the thirteenth international conference on artificial intelligence and statistics*, pp. 249–256. JMLR Workshop and Conference Proceedings, 2010.

Thomas L Griffiths, Frederick Callaway, Michael B Chang, Erin Grant, Paul M Krueger, and Falk Lieder. Doing more with less: meta-reasoning and meta-learning in humans and machines. *Current Opinion in Behavioral Sciences*, 29:24–30, 2019. ISSN 2352-1546. doi: https://doi.org/10.1016/j.cobeha.2019.01.005. URL https://www.sciencedirect.com/science/article/pii/S2352154618302122. Artificial Intelligence.

Moritz Hardt and Yu Sun. Test-time training on nearest neighbors for large language models. In *The Twelfth International Conference on Learning Representations*, 2024. URL https://openreview.net/forum?id=CNL2bku4ra.

Roee Hendel, Mor Geva, and Amir Globerson. In-context learning creates task vectors. In Houda Bouamor, Juan Pino, and Kalika Bali (eds.), *Findings of the Association for Computational Linguistics: EMNLP 2023*, pp. 9318–9333, Singapore, December 2023. Association for Computational Linguistics. doi: 10.18653/v1/2023.findings-emnlp.624. URL https://aclanthology.org/2023.findings-emnlp.624/.

Edward J Hu, yelong shen, Phillip Wallis, Zeyuan Allen-Zhu, Yuanzhi Li, Shean Wang, Lu Wang, and Weizhu Chen. LoRA: Low-rank adaptation of large language models. In *International Conference on Learning Representations*, 2022. URL https://openreview.net/forum?id=nZeVKeeFYf9.

Jinwu Hu, Zitian Zhang, Guohao Chen, Xutao Wen, Chao Shuai, Wei Luo, Bin Xiao, Yuanqing Li, and Mingkui Tan. Test-time learning for large language models. In *Forty-second International Conference on Machine Learning*, 2025. URL https://openreview.net/forum?id=iCYbIaGKSR.

Brandon Huang, Chancharik Mitra, Leonid Karlinsky, Assaf Arbelle, Trevor Darrell, and Roei Herzig. Multimodal task vectors enable many-shot multimodal in-context learning. In *The Thirty-eighth Annual Conference on Neural Information Processing Systems*, 2024. URL https://openreview.net/forum?id=W0okTgsPvM.

Justin Johnson, Bharath Hariharan, Laurens Van Der Maaten, Li Fei-Fei, C Lawrence Zitnick, and Ross Girshick. Clevr: A diagnostic dataset for compositional language and elementary visual reasoning. In *Proceedings of the IEEE conference on computer vision and pattern recognition*, pp. 2901–2910, 2017.

Adilbek Karmanov, Dayan Guan, Shijian Lu, Abdulmotaleb El Saddik, and Eric Xing. Efficient test-time adaptation of vision-language models. *The IEEE/CVF Conference on Computer Vision and Pattern Recognition*, 2024.

Louis Kirsch and Jürgen Schmidhuber. Self-referential meta learning. In *First Conference on Automated Machine Learning (Late-Breaking Workshop)*, 2022. URL https://openreview.net/forum?id=WAcLlCixQP7.

Ranjay Krishna, Yuke Zhu, Oliver Groth, Justin Johnson, Kenji Hata, Joshua Kravitz, Stephanie Chen, Yannis Kalantidis, Li-Jia Li, David A. Shamma, Michael S. Bernstein, and Li Fei-Fei. Visual genome: Connecting language and vision using crowdsourced dense image annotations. *International Journal of Computer Vision*, 123(1):32–73, May 2017. ISSN 1573-1405. doi: 10.1007/s11263-016-0981-7. URL https://doi.org/10.1007/s11263-016-0981-7.

Hugo Laurençon, Léo Tronchon, Matthieu Cord, and Victor Sanh. What matters when building vision-language models?, 2024. URL https://arxiv.org/abs/2405.02246.

Brian Lester, Rami Al-Rfou, and Noah Constant. The power of scale for parameter-efficient prompt tuning. In Marie-Francine Moens, Xuanjing Huang, Lucia Specia, and Scott Wen-tau Yih (eds.), *Proceedings of the 2021 Conference on Empirical Methods in Natural Language Processing*, pp. 3045–3059, Online and Punta Cana, Dominican Republic, November 2021. Association for Computational Linguistics. doi: 10.18653/v1/2021.emnlp-main.243. URL https://aclanthology.org/2021.emnlp-main.243/.

Bo Li, Yuanhan Zhang, Liangyu Chen, Jinghao Wang, Jingkang Yang, and Ziwei Liu. Otter: A multi-modal model with in-context instruction tuning, 2023a. URL https://arxiv.org/abs/2305.03726.

Bo Li, Yuanhan Zhang, Dong Guo, Renrui Zhang, Feng Li, Hao Zhang, Kaichen Zhang, Peiyuan Zhang, Yanwei Li, Ziwei Liu, and Chunyuan Li. LLaVA-onevision: Easy visual task transfer. *Transactions on Machine Learning Research*, 2025. ISSN 2835-8856. URL https://openreview.net/forum?id=zKv8qULV6n.

Juncheng Li, Minghe Gao, Longhui Wei, Siliang Tang, Wenqiao Zhang, Mengze Li, Wei Ji, Qi Tian, Tat-Seng Chua, and Yueting Zhuang. Gradient-regulated meta-prompt learning for generalizable vision-language models. In *2023 IEEE/CVF International Conference on Computer Vision (ICCV)*, pp. 2551–2562, 2023b. doi: 10.1109/ICCV51070.2023.00241.

Haotian Liu, Chunyuan Li, Qingyang Wu, and Yong Jae Lee. Visual instruction tuning. In *Thirty-seventh Conference on Neural Information Processing Systems*, 2023. URL https://openreview.net/forum?id=w0H2xGHlkw.

Haotian Liu, Chunyuan Li, Yuheng Li, and Yong Jae Lee. Improved baselines with visual instruction tuning. In *Proceedings of the IEEE/CVF Conference on Computer Vision and Pattern Recognition (CVPR)*, pp. 26296–26306, June 2024.

Pan Lu, Hritik Bansal, Tony Xia, Jiacheng Liu, Chunyuan Li, Hannaneh Hajishirzi, Hao Cheng, Kai-Wei Chang, Michel Galley, and Jianfeng Gao. Mathvista: Evaluating mathematical reasoning of foundation models in visual contexts. In *The Twelfth International Conference on Learning Representations*, 2024. URL https://openreview.net/forum?id=KUNzEQMWU7.

Sewon Min, Mike Lewis, Luke Zettlemoyer, and Hannaneh Hajishirzi. MetaICL: Learning to learn in context. In Marine Carpuat, Marie-Catherine de Marneffe, and Ivan Vladimir Meza Ruiz (eds.), *Proceedings of the 2022 Conference of the North American Chapter of the Association for Computational Linguistics: Human Language Technologies*, pp. 2791–2809, Seattle, United States, July 2022. Association for Computational Linguistics. doi: 10.18653/v1/2022.naacl-main.201. URL https://aclanthology.org/2022.naacl-main.201/.

Ivona Najdenkoska, Xiantong Zhen, and Marcel Worring. Meta learning to bridge vision and language models for multimodal few-shot learning. In *The Eleventh International Conference on Learning Representations*, 2023. URL https://openreview.net/forum?id=3oWo92cQyxL.

Chengwei Qin, Shafiq Joty, Qian Li, and Ruochen Zhao. Learning to initialize: Can meta learning improve cross-task generalization in prompt tuning? In Anna Rogers, Jordan Boyd-Graber, and Naoaki Okazaki (eds.), *Proceedings of the 61st Annual Meeting of the Association for Computational Linguistics (Volume 1: Long Papers)*, pp. 11802–11832, Toronto, Canada, July 2023. Association for Computational Linguistics. doi: 10.18653/v1/2023.acl-long.659. URL https://aclanthology.org/2023.acl-long.659/.

Qwen, :, An Yang, Baosong Yang, Beichen Zhang, Binyuan Hui, Bo Zheng, Bowen Yu, Chengyuan Li, Dayiheng Liu, Fei Huang, Haoran Wei, Huan Lin, Jian Yang, Jianhong Tu, Jianwei Zhang, Jianxin Yang, Jiaxi Yang, Jingren Zhou, Junyang Lin, Kai Dang, Keming Lu, Keqin Bao, Kexin Yang, Le Yu, Mei Li, Mingfeng Xue, Pei Zhang, Qin Zhu, Rui Men, Runji Lin, Tianhao Li, Tianyi Tang, Tingyu Xia, Xingzhang Ren, Xuancheng Ren, Yang Fan, Yang Su, Yichang Zhang, Yu Wan, Yuqiong Liu, Zeyu Cui, Zhenru Zhang, and Zihan Qiu. Qwen2.5 technical report, 2025. URL https://arxiv.org/abs/2412.15115.

Sachin Ravi and Hugo Larochelle. Optimization as a model for few-shot learning. In *International Conference on Learning Representations*, 2017. URL https://openreview.net/forum?id=rJY0-Kcll.

ShareGPT. Sharegpt. https://sharegpt.com/, 2023.

Manli Shu, Weili Nie, De-An Huang, Zhiding Yu, Tom Goldstein, Anima Anandkumar, and Chaowei Xiao. Test-time prompt tuning for zero-shot generalization in vision-language models. In Alice H. Oh, Alekh Agarwal, Danielle Belgrave, and Kyunghyun Cho (eds.), *Advances in Neural Information Processing Systems*, 2022. URL https://openreview.net/forum?id=e8PVEkSa4Fq.

Amanpreet Singh, Guan Pang, Mandy Toh, Jing Huang, Wojciech Galuba, and Tal Hassner. Textocr: Towards large-scale end-to-end reasoning for arbitrary-shaped scene text. In *Proceedings of the IEEE/CVF conference on computer vision and pattern recognition*, pp. 8802–8812, 2021.

Maria Tsimpoukelli, Jacob L Menick, Serkan Cabi, S. M. Ali Eslami, Oriol Vinyals, and Felix Hill. Multimodal few-shot learning with frozen language models. In M. Ranzato, A. Beygelzimer, Y. Dauphin, P.S. Liang, and J. Wortman Vaughan (eds.), *Advances in Neural Information Processing Systems*, volume 34, pp. 200–212. Curran Associates, Inc., 2021. URL https://proceedings.neurips.cc/paper_files/paper/2021/file/01b7575c38dac42f3cfb7d500438b875-Paper.pdf.

Ashish Vaswani, Noam Shazeer, Niki Parmar, Jakob Uszkoreit, Llion Jones, Aidan N Gomez, Łukasz Kaiser, and Illia Polosukhin. Attention is all you need. *Advances in neural information processing systems*, 30, 2017.

Oriol Vinyals, Charles Blundell, Timothy Lillicrap, Koray Kavukcuoglu, and Daan Wierstra. Matching networks for one shot learning. In *Proceedings of the 30th International Conference on Neural Information Processing Systems*, NIPS'16, pp. 3637–3645, Red Hook, NY, USA, 2016. Curran Associates Inc. ISBN 9781510838819.

Lilian Weng. Meta-learning: Learning to learn fast. https://lilianweng.github.io/posts/2018-11-30-meta-learning/, 2018.

Mitchell Wortsman, Gabriel Ilharco, Samir Yitzhak Gadre, Rebecca Roelofs, Raphael Gontijo-Lopes, Ari S. Morcos, Hongseok Namkoong, Ali Farhadi, Yair Carmon, Simon Kornblith, and Ludwig Schmidt. Model soups: averaging weights of multiple fine-tuned models improves accuracy without increasing inference time, 2022. URL https://arxiv.org/abs/2203.05482.

Sangdoo Yun, Dongyoon Han, Sanghyuk Chun, Seong Joon Oh, Youngjoon Yoo, and Junsuk Choe. Cutmix: Regularization strategy to train strong classifiers with localizable features. In *2019 IEEE/CVF International Conference on Computer Vision (ICCV)*, pp. 6022–6031, 2019. doi: 10.1109/ICCV.2019.00612.

Xiaohua Zhai, Basil Mustafa, Alexander Kolesnikov, and Lucas Beyer. Sigmoid loss for language image pre-training, 2023. URL https://arxiv.org/abs/2303.15343.

Hongyi Zhang, Moustapha Cisse, Yann N. Dauphin, and David Lopez-Paz. mixup: Beyond empirical risk minimization. In *International Conference on Learning Representations*, 2018. URL https://openreview.net/forum?id=r1Ddp1-Rb.

Haozhe Zhao, Zefan Cai, Shuzheng Si, Xiaojian Ma, Kaikai An, Liang Chen, Zixuan Liu, Sheng Wang, Wenjuan Han, and Baobao Chang. MMICL: Empowering vision-language model with multimodal in-context learning. In *The Twelfth International Conference on Learning Representations*, 2024. URL https://openreview.net/forum?id=5KojubHBr8.

Yongshuo Zong, Ondrej Bohdal, and Timothy Hospedales. VL-ICL bench: The devil in the details of multimodal in-context learning. In *The Thirteenth International Conference on Learning Representations*, 2025. URL https://openreview.net/forum?id=cpGPPLLYYx.

A APPENDIX

A.1 Implementation Details

A.1.1 Finetuning Data Mixture

For model finetuning, we create our multi-task data mixture for single image per example using the visual instruction tuning data of LLaVA v1.5 (Liu et al., 2023) which contains a mixture of 12 different datasets[6] ranging from long conversations to academic multiple-choice questions. Since we are only training image-based prompts, we remove the language-only ShareGPT-40K dataset (ShareGPT, 2023). Additionally, we include 3 different math reasoning/QA datasets from the LLaVA OneVision data mixture (Li et al., 2025) which are known to improve LMM performance on difficult reasoning and logical QA tasks (Lu et al., 2024). We further get rid of the extra answer formatting instructions to test the true few-shot transfer learning ability of our approach without the need of external task induction. Table 4 shows the list of all the datasets along with their size and question types.

Table 4: Finetuning Data Mixture Statistics

Dataset	No. of examples	Question Types
LLaVA-Instruct	157,712	Conversations (57,669) Detailed Image Description (23,240) Complex Reasoning (76,803)
GQA	72,140	Visual Reasoning
OCR-VQA	80,000	Image Question Answering with Reading Comprehension
TextVQA	21,953	Image Question Answering with Reading Comprehension
Visual Genome	86,417	Image Question Answering and Bounding Box Prediction
MAVIS-Math-Metagen	87,348	Visual Math Question Answering
TabMWP-Cauldron	22,717	Tabular Math Reasoning
RefCOCO	48,447	Image Question Answering and Bounding Box Prediction
OKVQA	8,998	Knowledge Grounded Image Question Answering
VQAv2	82,783	Image Question Answering
A-OKVQA	66,160	Multiple-Choice Question Answering
Geo-170k (QA)	67,823	Math Question Answering and Reasoning
Total	802,498	

A.1.2 Model Configurations

Models We use the publicly available implementation of LLaVA v1.5[7] and first-order MAML[8] to implement our baselines. Additionally, we use the pretrained model weights from Huggingface for

[6]We use this dataset only for academic research purposes as mentioned by the original authors and follow the Open AI Usage Policy for GPT-4 generated datasets. Additionally, we conform to the license (CC-BY-4.0) for Cauldron datasets.

[7]LLaVA v1.5: `https://github.com/haotian-liu/LLaVA/tree/main/llava`

[8]MAML: `https://github.com/AntreasAntoniou/HowToTrainYourMAMLPytorch`

Qwen2.5-7B-Instruct LLM[9] and the CLIP ViT-L/14-336px visual encoder[10]. The output embedding dimension size of CLIP is 1,024 and the input word embedding size of the Qwen LLM is 3,584. We set the training context length as 4096 for all baselines except for in-context baseline where it is 8,192 as it requires training with longer sequences. The attention-mapper is a single multi-head attention block with 8 heads. The token length of the soft prompt P as described in Section 3.3 for the attention mapper is set to $m = 256$. The total number of trainable parameters for our model is approximately 24M making our approach significantly parameter-efficient for finetuning.

A.1.3 Training Details

Pretraining stage During the pretraining stage, we only train the attention-mapper and soft prompts for 4 epochs and use a learning rate of 2e-3 with a batch size of 64 per GPU. We perform a train-validation split on the LCS-558K dataset (Liu et al., 2023) by keeping 98% of the examples for training and 2% for validation and take the checkpoint with the lowest validation loss. We use this checkpoint as our base for further task-specific finetuning.

Finetuning stage For finetuning, in order to keep a balanced ratio of train-validation splits across multiple datasets in Section A.1.1 used in this stage, we divide each dataset into 98% for training and 2% for validation and then combine them separately to create the final train and validation splits. We experimented among three different learning rates [1e-3, 5e-4, 2e-5]. For MAPD, we further experimented with three different inner-loop learning rates [1e-1, 5e-2, 5e-1]. Below, we mention the best learning rates along with other hyperparameters, chosen using our validation set for the different approaches proposed in Section 3.4 and LoRA (Hu et al., 2022). All approaches were finetuned for 1 epoch to ensure a complete pass over the entire finetuning data mixture.

1. **MAPD:** We use 5 inner-loop steps and initialize the inner-loop learning rate α=1e-1. The outer-loop learning rate is set as 1e-3 with a per GPU batch size of 1 meta-task with a gradient accumulation of 2 steps. Each meta-task here contains 10 support and 10 query examples. Training time $\sim$ 10 hours.
2. **Multi-Task$^{\text{PD}}$:** Similar to MAPD, we use a learning rate of 1e-3 with a per GPU batch size of 1 meta-task with a gradient accumulation of 4 steps. Each meta-task here contains 5 support and 5 query examples. Training time $\sim$ 4.5 hours
3. **In-Context$^{\text{PD}}$:** We use a learning rate of 1e-3 with a gradient accumulation of 4 steps and 5 meta tasks per GPU. Each meta task contains 10 support examples and 1 query example. The support examples were concatenated with the strategy that ensured all image tokens of a meta-task are present in the sequence and we truncate the text tokens if the sequence exceeded the context length of 8192. Further, the few-shot question and answers were concatenated by inserting "Question:" and "Answer:" strings in between them, inspired from (Alayrac et al., 2022). Training time $\sim$ 4.5 hours
4. **ModelAvg$^{\text{PD}}$:** We first finetune individual models on each dataset in the finetuning data mixture (Section A.1.1) with a learning rate of 5e-4. For all the datasets, we choose a per GPU batch size of 8 with gradient accumulation of 2 steps. Average time per dataset $\sim$ 3 hours
5. **NoMeta-task$^{\text{PD}}$:** Here, we finetune on the complete data mixture in one training run by sampling batches randomly and again use a per GPU batch size of 8 with a gradient accumulation of 2 steps. We also use a learning rate of 5e-4. Training time $\sim$ 4 hours.
6. **LoRA**: We only apply LoRA to the attention matrices (Q, K, V) of each layer. For training, we use a learning rate of 5e-4 and a per GPU batch size of 8 with gradient accumulation of 2 steps. Further, we performed hyperparameter search for choosing LoRA parameters - rank (r) and scaling factor (α) for the three settings shown in Table 2. Training time $\sim$ 4 hours.
   (a) *All LLM layers* ($r = 128, \alpha = 256$)
   (b) *[0-15] LLM layers* ($r = 16, \alpha = 64$)
   (c) *[0-15] LLM layers + ATT*: ($r = 16, \alpha = 64$)

[9]Qwen2.5-7B-Instruct: `https://huggingface.co/Qwen/Qwen2.5-7B-Instruct`
[10]CLIP-ViT-L/14-336px: `https://huggingface.co/openai/clip-vit-large-patch14-336`

Computational Requirements We find that the GPU requirement for training the attention-mapper mostly depends on the size of the underlying LLM used. For the 7B model training, we use 4 H200 GPUs with a VRAM of 143GB per GPU and for 3B models only 2 H200 GPUs were needed. For both the stages, the hyperparameters were tuned using their corresponding validation sets and we choose the checkpoints at the end of first epoch to report our results.

A.1.4 PSEUDO ALGORITHM FOR MAPD

We highlight our full MAPD algorithm based on FoMAML in detail with inner and outer loop that is used to train the attention-mapper parameters θ_p in Algorithm 1.

Algorithm 1: Meta-Adaptive Prompt Distillation (MAPD)

Input: Meta-Task distribution $p(\mathcal{T}^{\text{meta}})$, inner-loop learning rate α, meta learning rate β
Output: Meta-parameters $\theta_p = \{\theta, P\}$
Initialize θ_p with Xavier Uniform Initialization;
while *not converged* **do**
  Sample batch of meta-tasks $\{T_j\}_{j=1}^{N} \sim p(\mathcal{T}^{\text{meta}})$;
  foreach *task* $T_j = \{D_j^{supp}, D_j^{query}\}$ *in batch* **do**
    Evaluate $L^{\text{supp}}_{\theta_{p,j}} = \frac{-1}{|D_j^{\text{supp}}|} \sum_{i=1}^{|D_j^{\text{supp}}|} \log(p_{\theta_{p,j}}(X_a^i | X_v^i, X_q^i))$;
    Adapt parameters with K gradient steps:
    for $k = 1, \ldots, K$ **do**
      $$\theta_{p,j}^{k} \leftarrow \theta_{p,j}^{k-1} - \alpha \nabla_{\theta_{p,j}^{k-1}} L^{\text{supp}}_{\theta_{p,j}^{k-1}}$$
  Evaluate $L^{\text{query}}_{\theta^K_{p,j}} = \frac{-1}{|D_j^{\text{query}}|} \sum_{i=1}^{|D_j^{\text{query}}|} \log(p_{\theta^K_{p,j}}(X_a^i | X_v^i, X_q^i))$;
  First-Order Meta-Update:
  $$\theta_p \leftarrow \theta_p - \beta \sum_{j=1}^{N} \nabla_{\theta^K_{p,j}} L^{\text{query}}_{\theta^K_{p,j}}$$

A.2 EVALUATION DETAILS

Table 5: Evaluation Dataset Statistics

Dataset	Task Category	Train Set (Support)	Test Set (Query)	Size (GB)
Fast Open-MiniImageNet (OPEN_MI)	Fast-Concept Binding	5,000	200	0.18
CLEVR Count Induction	Fine-Grained Perception, Task Induction	800	200	0.18
Operator Induction	Perception, Task Induction Mathematical Reasoning	80	60	0.01
TextOCR	Perception, Task Induction	800	200	0.01

A.2.1 EVALUATION DATASETS FROM VL-ICL BENCH

The VL-ICL Bench Zong et al. (2025) includes a diverse variety of tasks to test different capabilities of models like Fast-Concept binding, Mathematical Induction, and Fine-grained perception. Given the nature of our model architecture and training (Section 3), we only focus on the single-image

Figure 5: 2-way Fast Open-Ended MiniImageNet

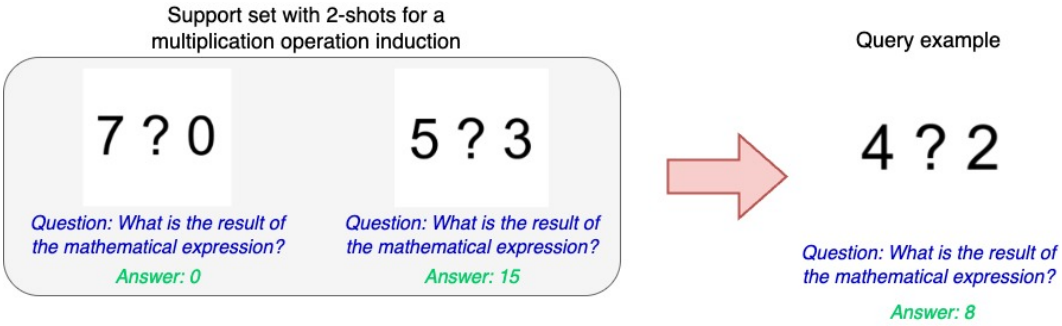

Figure 6: Operator Induction

Image-to-text (I2T) tasks. Table 5 shows the dataset statistics. We also give brief descriptions of these tasks below along with some examples for better understanding.

1. **Fast Open-Ended MiniImageNet (OPEN_MI)** - This is a variant of the MiniImageNet few-shot object recognition task (Vinyals et al., 2016), which was repurposed for few-shot prompting (Tsimpoukelli et al., 2021). It is essentially an open-ended image classfication problem, but contains nonsense categorical names like *dax* or *blicket* making the test performance not influenced by the prior knowledge of an LMM but only dependent on the support examples. This design ensures to test the few-shot abilities of LMMs and how quickly they can learn about new concepts. For the results shown in Table 7, we use the 2-way version of this task involving classification between two nonsense categories. An example of a 2-way 1-shot task is shown in Figure 5.
2. **Operator Induction** - Initially proposed by (Zong et al., 2025), this dataset tests various capabilties of LMMs like Task Induction, Perception and Mathematical Reasoning. The support examples involve two operands with a missing mathematical operation and an answer. When testing, the task is to identify the hidden operation from the support example and use it to calculate the result over the operands in the query. An example of a 2-shot task is shown in Figure 6.
3. **CLEVR Count Induction** - This dataset contains images from the widely used CLEVR dataset (Johnson et al., 2017) where each image contains a set of objects that have certain characteristics based on attributes like shape, size, color and material. The task is to learn to count the objects of the given attribute in the support example and transfer that knowledge to count the objects of any attribute in the query example. An example of a 2-shot task is shown in Figure 7.
4. **TextOCR** - This dataset has been repurposed by (Zong et al., 2025) from the TextOCR dataset (Singh et al., 2021) to create a task where the LMM should learn to output the text within a red bounding box from the support examples. Even though this task could be solved in a zero-shot setting as we see in the 0-shot case with a detailed prompt, we still only focus on inducing task knowledge from the few-shot examples. An example of a 2-shot task is shown in Figure 8.

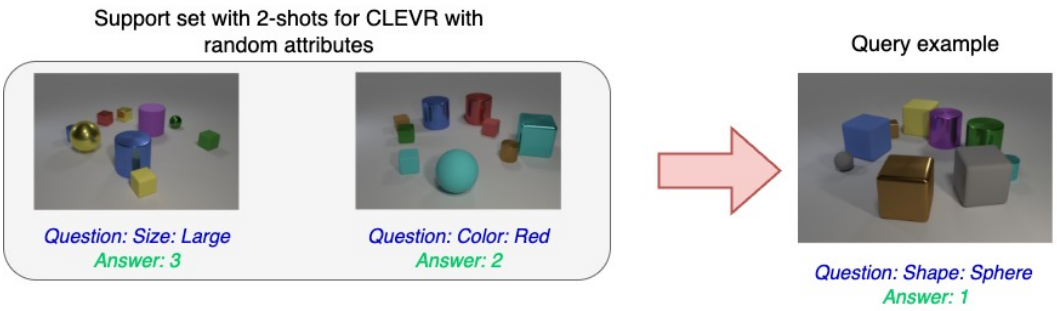

Figure 7: CLEVR Count Induction

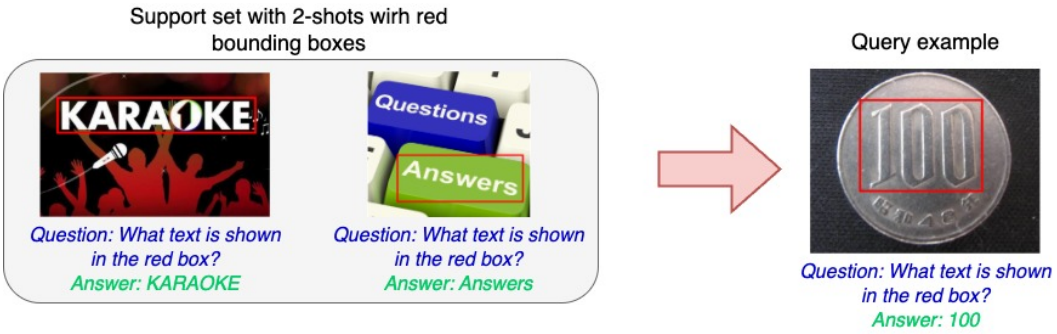

Figure 8: TextOCR

A.2.2 Test-Time Adaptation Details

We choose a similar test-time adaptation procedure as (Qin et al., 2023) to find the best hyperparameter settings for every prompt distillation method for fair comparison. We first sample 10% of the examples from the training split of each test task and combine them to create a validation set. After meta-task creation of VL-ICL datasets (Zong et al., 2025) using the remaining training and test splits, we then performed a maximum of $K = 30$ inner-loop steps over each support set of a meta-task and chose the Kth-step model that gave the lowest validation loss. We use this model to calculate the result over the query set. To further show how the performance varies at different gradient steps, we plot the average test accuracy curves for different VL-ICL datasets for MAPD for different shots in Figure 9. We see that the accuracies converge or start decreasing under 30 gradient steps which validates our adaptation procedure designed to achieve best performance. We have also provided examples of how the predictions change during test-time adaptation in Figure 10, Figure 11, Figure 12, and Figure 13. Further to ensure reproducibility, we provide our best learning rate values in Table 6 used for different methods based on the validation set after doing a hyperparameter search within the range $[0.1, 1.0]$ with a batch size of 1 meta-task.

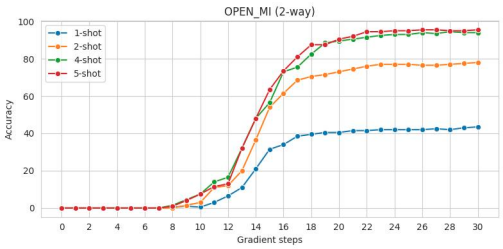

(a) OPEN_MI test performance

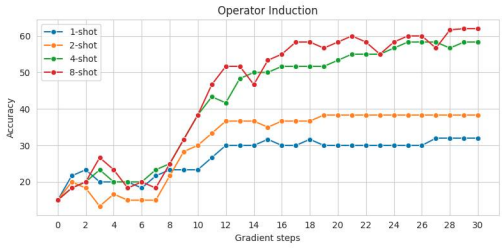

(b) Operator Induction test performance

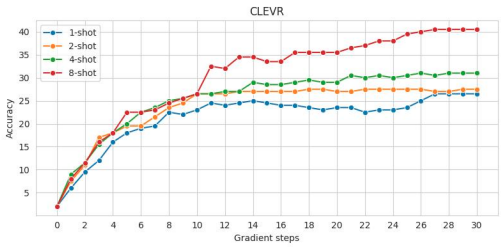

(c) CLEVR test performance

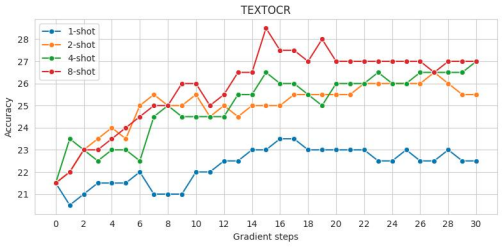

(d) TEXTOCR test performance

Figure 9: Average test performances of MAPD with finetuning on different datasets

Table 6: Learning rates for finetuning-based (FT) test-time adaptation for results shown in Table 1, Table 2, Table 7 and Table 8.

Training Methods	Learning Rate (LR)
MAPD	1.0
Multi-Task^{PD}	0.8
In-Context^{PD}	0.8
ModelAvg^{PD}	0.6
NoMeta-task^{PD}	1.0
LoRA	0.2

A.2.3 DETAILED RESULTS

Table 7: Comparison of different prompt distillation approaches on single-image tasks from VL-ICL Bench (Zong et al., 2025). We report accuracy for different numbers of shots (–S). "Avg" is only calculated for ≥ 1 shot(s). FT = Finetuning with ≤ 30 gradient steps, ICL = In-Context Learning, TTA= Test-Time Adaptation. More details are mentioned in Appendix A.2.2. We do not compare on 0-shot results. The model used for this evaluation is LLaVA-ATT-Qwen2.5 7B which is described in Section 3.3. Meta-Tasks used (✓) or not (✗) during training. We also provide results for higher number of shots in Appendix A.2.9 and qualitative results in Appendix A.2.5 and A.2.8.

Methods	Meta Task	Open-MI (2-way)						Operator Induction					
		0-S	1–S	2–S	4–S	5-S	Avg	0-S	1–S	2–S	4–S	8–S	Avg
TTA with ICL													
NoMeta-task^{PD}	✗	0.0	35.0	47.0	48.0	45.0	43.8	11.7	13.3	13.3	10.0	11.7	12.1
Model-Avg^{PD}	✗	0.0	20.0	22.0	30.0	34.5	26.6	8.3	11.7	6.7	8.3	10.0	9.2
In-Context^{PD}	✓	0.0	30.0	56.0	55.0	63.5	51.1	10.0	20.0	18.5	18.0	26.0	20.6
Multi-Task^{PD}	✓	0.0	43.0	50.0	51.0	50.5	48.6	8.3	13.3	11.7	3.3	11.7	10.0
MAPD	✓	0.0	42.5	53.0	57.0	60.5	53.3	15.0	13.3	13.3	1.7	10.0	9.6
TTA with FT $\leq$30													
NoMeta-task^{PD}	✗	0.0	21.5	67.5	89.0	94.0	68.0	11.7	26.7	23.3	46.7	58.3	38.8
Model-Avg^{PD}	✗	0.0	28.5	53.5	83.0	87.5	63.1	8.3	31.5	28.0	45.0	55.5	40.0
In-Context^{PD}	✓	0.0	35.5	54.5	79.5	88.5	64.5	10.0	21.7	18.3	41.7	41.7	30.9
Multi-Task^{PD}	✓	0.0	37.0	73.5	93.5	94.5	74.6	8.3	31.0	28.3	**61.0**	60.0	45.1
MAPD	✓	0.0	**43.5**	**78.0**	**94.5**	**95.5**	**77.9**	15.0	**32.0**	**38.3**	58.3	**62.0**	**47.7**

Methods	Meta Task	CLEVR Count Induction						TextOCR					
		0–S	1–S	2–S	4–S	8-S	Avg	0-S	1–S	2–S	4–S	8–S	Avg
TTA with ICL													
NoMeta-task^{PD}	✗	0.0	8.0	10.5	23.0	30.5	18.0	20.0	4.5	9.5	8.5	4.5	6.8
Model-Avg^{PD}	✗	1.5	17.0	8.5	4.0	1.0	7.6	12.0	3.0	2.5	3.0	1.0	2.8
In-Context^{PD}	✓	0.0	13.5	23.0	28.5	31.5	24.1	16.0	22.5	21.0	23.5	28.0	23.8
Multi-Task^{PD}	✓	1.0	5.0	9.0	16.5	19.5	12.5	18.0	4.0	4.5	8.5	10.5	6.9
MAPD	✓	2.0	11.0	7.0	15.5	15.5	12.3	21.5	5.5	7.0	8.0	8.5	7.3
TTA with FT $\leq$30													
NoMeta-task^{PD}	✗	0.0	18.5	21.5	26.0	37.0	25.8	20.0	20.5	23.0	24.0	22.5	22.5
Model-Avg^{PD}	✗	1.5	**26.5**	25.0	29.5	35.5	29.1	12.0	17.5	20.0	23.0	25.5	21.5
In-Context^{PD}	✓	0.5	24.5	**30**	**34.5**	34.5	30.9	16.0	16.0	18.0	19.5	22.0	18.9
Multi-Task^{PD}	✓	0.0	25.0	25.5	31.0	38.0	29.9	18.0	21.0	20.5	24.5	25.5	22.9
MAPD	✓	0.0	**26.5**	27.5	31.0	**40.5**	**31.4**	21.5	**23.5**	**26.5**	**27.0**	**28.5**	**26.4**

Table 8: Comparison of the LoRA baselines on VL-ICL Bench (Zong et al., 2025). "Avg" is only calculated for ≥ 1 shot(s) (-S). TTA= Test-Time Adaptation. FT=Finetuning with ≤ 30 gradient steps. ATT=Attention-Mapper. The model used for this evaluation is LLaVA-ATT-Qwen2.5 7B.

LoRA	Open-MI (2-way)						Operator Induction					
	0-S	1–S	2–S	4–S	5-S	Avg	0-S	1–S	2–S	4–S	8–S	Avg
TTA with FT $\leq$ 30												
All LLM layers	0.0	24.5	45.7	68.3	81.9	55.1	8.1	11.7	10.0	13.3	18.2	13.3
[0-15] LLM layers	0.0	30.9	**65.3**	81.1	**91.9**	67.3	8.3	18.3	26.3	23.1	34.3	25.5
[0-15] LLM layers + ATT	0.0	**37.3**	64.1	**83.5**	91.5	**69.1**	10.0	**21.5**	**28.3**	**35.5**	**36.7**	**30.5**

LoRA	CLEVR Count Induction						TextOCR					
	0-S	1–S	2–S	4–S	5-S	Avg	0-S	1–S	2–S	4–S	8–S	Avg
TTA with FT $\leq$ 30												
All LLM layers	0.0	9.3	11.7	15.5	23.9	15.1	15.0	6.7	9.1	13.3	12.5	10.4
[0-15] LLM layers	0.0	21.5	**28.3**	**32.5**	**37.7**	**30.0**	18.3	20.3	**24.5**	25.5	24.9	23.8
[0-15] LLM layers + ATT	0.0	**26.0**	23.1	30.0	35.7	28.7	18.3	**20.6**	23.4	**26.5**	**27.5**	**24.5**

A.2.4 PERFORMANCE OF PUBLICLY AVAILABLE LMMS ON VL-ICL BENCH

Table 9: Performance of different LMMs on single-image tasks from VL-ICL Bench. We report the "Avg" accuracy for different numbers of shots - $\{1, 2, 4, 5, 8\}$. FT = Finetuning with ≤ 30 gradient steps, ICL = In-Context Learning, TTA= Test-Time Adaptation, VL-Data=Vision-Language Data, LAQ-7B=LLaVA-ATT-Qwen2.5-7B, CLIP=CLIP-ViT-L/14-336px, MLP=2-layer MLP, ATT=Attention-Mapper. **Bold** shows best performance.

Methods	VL-Data	Params trained	TTA	Open-MI	OP_IND	CLEVR	TextOCR
LLaVA v1.5-7B	1.2M	7B	ICL	12.4	5.4	10.9	4.4
LLaVA-Next-7B	1.3M	7.06B	ICL	34.4	5.4	21.1	0.4
LLaVA-OneVision-7B	10.4M	8B	ICL	42.1	41.7	34.9	42.3
LLaVA-OneVision-72B	10.4M	73.2B	ICL	75.1	69.1	**37.2**	**52.2**
Qwen2-VL-7B-Instruct	-NA-	8B	ICL	73.5	69.6	27.9	50.5
Qwen2.5-VL-7B-Instruct	-NA-	8B	ICL	44.0	**84.2**	22.0	36.9
LAQ-7B + In-Context^{PD}	1.3M	24M	ICL	51.1	20.6	24.1	23.8
LAQ-7B + In-Context^{PD}	1.3M	24M	FT$\leq$30	64.5	30.9	30.9	18.9
LAQ-7B + MAPD	1.3M	24M	ICL	53.3	9.6	12.3	7.3
LAQ-7B + MAPD	1.3M	24M	FT$\leq$30	**77.9**	47.7	31.4	26.4

We show performance of publicly available LMMs and our best performing LMM architecture (LLaVA-ATT-Qwen2.5-7B) on the single-image tasks from VL-ICL Bench in Table 9. We only provide this as a reference and note that its not possible to directly compare different LMMs due to their fundamental differences in model architectures, sizes and training datasets. We see that our model along with MAPD based meta-learning and finetuning-based adaptation performs comparably with other publicly available LMMs and even surpasses LLaVA-OneVision-72B ICL performance for the Fast Open-Ended MiniImageNet (Open-MI) task and other 7B LLaVA and Qwen-VL models on other tasks. Note that unlike other LMMs, LLaVA-ATT-Qwen2.5 does not finetune the LLM in complete training and uses significantly lesser vision-language data (1.3M) and trainable parameters (24M) compared to LLaVA-OneVision that trains the complete model with 10.4M examples. This shows promising results regarding the data and parameter efficiency of our prompt distillation approach MAPD, which achieves state-of-the-art performance on Open-MI with finetuning just the attention-mapper with upto 30 gradient steps on the few-shot examples.

A.2.5 QUALITATIVE RESULTS

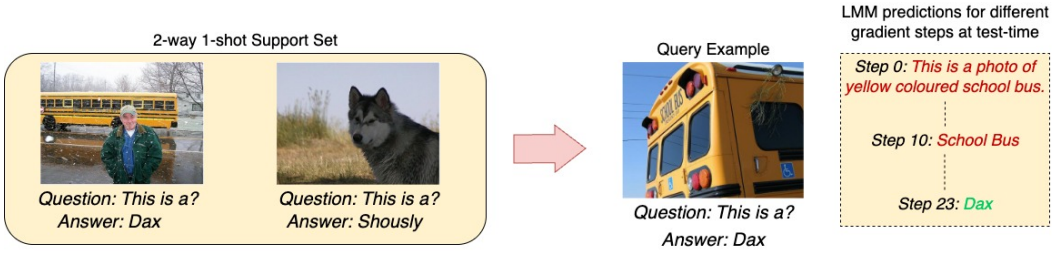

Figure 10: OPEN_MI predictions at test-time

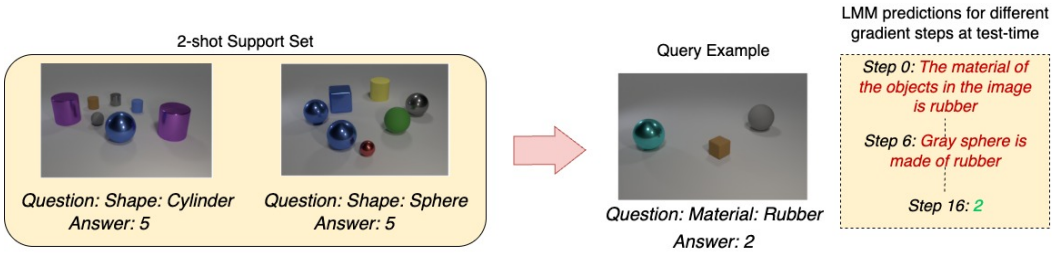

Figure 11: CLEVR predictions at test-time

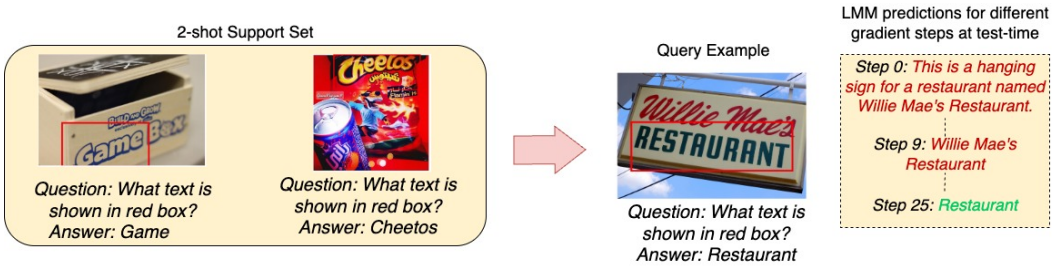

Figure 12: TEXTOCR predictions at test-time

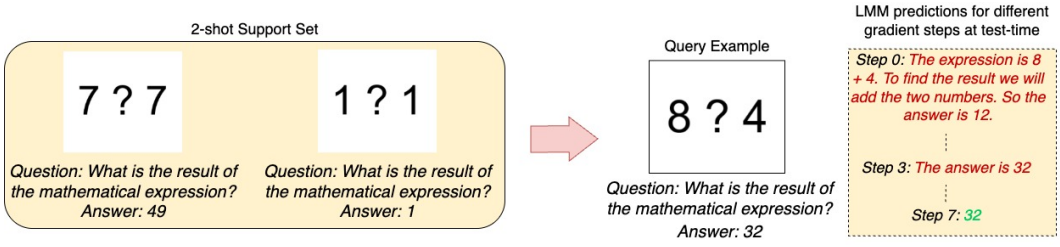

Figure 13: Operator Induction predictions at test-time

A.2.6 ROBUSTNESS AGAINST IMAGE PERTURBATIONS

Table 10: Robustness of prompt distillation methods against image perturbations on the Fast Open-Ended MiniImageNet dataset (2-way classification) for LLaVA-ATT-Qwen2.5 7B LMM. We report accuracy scores as defined in VL-ICL Bench (Zong et al., 2025) across 2, and 5 shots. Test-Time Adaptation = Finetuning with ≤ 30 gradient steps.

	NoMeta-task^{PD}		Model-Avg^{PD}		In-Context^{PD}		Multi-task^{PD}		MAPD	
	2–S	5–S	2–S	5–S	2–S	5-S	2–S	5–S	2–S	5–S
Original	67.5	94.0	53.5	87.5	54.5	88.5	73.5	94.5	78.0	95.5
Cropping	65.0	94.0	51.5	87.5	51.5	83.0	72.0	91.5	76.5	95.0
Rotation	67.0	91.0	50.5	81.5	50.5	83.5	72.5	93.5	78.0	95.5
Gaussian Blur	67.5	92.5	51.5	84.5	49.5	78.0	71.5	92.5	77.5	96.0
Color Jitter	66.5	92.5	50.5	89.0	49.5	81.5	71.5	94.0	77.0	94.0
CutMix	58.5	86.0	45.5	70.5	49.0	75.0	72.0	92.0	75.5	92.5
MixUp	58.0	84.0	46.0	70.5	48.0	75.5	69.0	89.0	76.5	91.0
Mean Drop in Accuracy	−3.8	−4.0	−4.3	−6.9	−4.8	−9.1	−2.1	−2.4	−1.2	−1.4
Net Mean Drop across Shots	−3.9		−5.6		−7.0		−2.3		**−1.3**	

We assess if our prompt distillation methods are robust enough to handle perturbations applied to the images in the support set as shown in Table 10. We see that our method, MAPD, is most robust even in the presence of noise in the support examples as compared to other distillation methods that suffer a huge drop in performance. Advanced techniques like CutMix (Yun et al., 2019) and MixUp (Zhang et al., 2018) change the original image distribution substantially, affecting all methods to a greater degree but MAPD is still close to its original performance for both 2 and 5 shots. This robustness likely stems from MAPD's meta-learned initialization, which learns the underlying task structure from meta-tasks without over-fitting to any other spurious visual patterns and this allows it to adapt quickly to newer tasks without being influenced by noisy visual artifacts in the examples.

A.2.7 HOW TO SELECT FEW-SHOT EXAMPLES FOR BETTER PERFORMANCE?

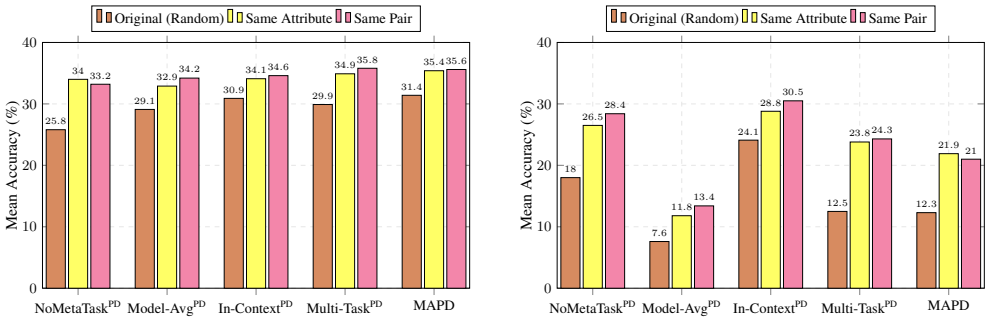

Figure 14: (a) Performance comparison of different prompt distillation approaches on the CLEVR Count Induction (details in Appendix A.2.1). Few-shot examples for *Same Attribute* and *Same Pair* are selected based on their *attribute-value* similarity with the query (test) example. Mean Accuracy is computed for 1,2,4 and 8 shots. **Left**: Finetuning (FT) based Test-time Adaptation. (b) **Right**: In-Context Learning (ICL) based Test-time Adaptation.

We further assess how performance varies for different prompt distillation approaches based on the selection of few-shot examples on the CLEVR Count Induction task (details in Appendix A.2.1) as an example. We propose two selection methods based on similarity of attributes and their corresponding values for every query (test) example. If the query has attribute and value as *shape: sphere*, we select the few-shot examples based on - a) Same Attribute - *shape*, (b) Same Pair - *shape: sphere* and compare both of them with the original setup as proposed in the VL-ICL benchmark (Zong et al., 2025) which retrieves the few-shot examples randomly. In Figure 14(a), we first see that for finetuning-based (FT) adaptation, the performance of all the baselines increases by 4.8% for

Same Attribute and 5.3% for Same Pair on an average. MAPD performs best in the Same Attribute setting (Mean Acc = 35.4%) and Multi-Task^{PD} performing best in the Same Pair setting (Mean Acc = 35.8%). In Figure 14(b), we see that for In-Context Learning (ICL) adaptation, the similarity-based few-shot selection methods have a greater impact in performance and improve the mean accuracy of all the baselines by 7.7% for Same Attribute and 8.6% for Same Pair on an average. In-Context^{PD} performs the best in both Same Attribute and Same Pair settings with mean accuracies of 28.8% and 30.5% respectively for ICL adaptation. We also notice that the Same Pair setup is generally the best few-shot selection method giving best performance for all the approaches. This indicates that choosing few-shot examples that are similar to query example induces better task understanding during test-time adaptation. We also see that the selection of few-shot examples shows less variance with FT adaptation compared to ICL adaptation, thereby showing higher robustness of FT adaptation.

A.2.8 Details on Ablation Study for Operator Induction

We break down the ablation study on operator induction tasks (Section 4.3; Figure 4(b)) into 3 components: 1) Task Induction, 2) Perception, and 3) Mathematical Reasoning. We test these components separately with the help of suitable prompts for our LMM to answer questions in specific formats. Figure 15 shows our prompts used for different components.

- **Task Induction** - *"What mathematical operation should be used in this example? Strictly answer in one word."*
- **Perception** - *"What are the numbers in this example? Do not calculate the answer after applying mathematical operation. Only give the numbers shown in the example. Stricly give numbers in numeric digits and your result should be in the format > Number A: xxx || Number B: xxx."*
- **Mathematical Reasoning** - *"Think step-by-step and give proper reasoning steps first and then given your final answer. The format should be > Reasoning: xxx || Answer: xxx . The Reasoning part should contain reasons to derive the answer and the Answer part should only contain the answer. Your response should strictly follow this format and not just give the answer of the mathematical operation. It's important that you give reasoning before you answer."*

Figure 15: (Operator Induction Task) Prompts to the LMM for generating answers in specific formats suited for evaluation.

We list out a few examples which we curate for the Operator Induction task to enhance mathematical reasoning. Each image in the dataset contains a set of 2 numbers or operands and a hidden mathematical operation. The result of the correct mathematical operation is also provided for the support set examples. The task is to induce the mathematical operation used in the support set to calculate the answer of the query image containing two new operands. As finetuning on a single answer token limits the token generation capacity of the LMM, we further modify the support set examples to list out detailed mathematical steps before calculating the answer. Finetuning on this reasoning data improves both the generation capacity and reasoning ability of the LMM. We further provide a few examples of this hand-curated data in Figure 16.

We used Qwen2.5VL-32B-Instruct (Qwen et al., 2025) as a judge for evaluating the Mathematical Reasoning component of the problem where LMMs responded with detailed reasoning steps before the answer. Evaluation of responses was done by prompting the judge to score a response between 0–3 based on if it thinks the reasoning and answer are correct. We then calculated mean score as the percentage of total score assigned by the Qwen-2.5-VL (Judge) to the responses relative to the maximum possible score.

$$\text{Mean Percent Score} = \frac{\sum_{i=1}^{N} S_i}{3 * N} \times 100 \tag{9}$$

where S_i is the score assigned by Qwen2.5-VL for the ith response and N is the total number of responses. We provide the prompt to the judge for this evaluation in Figure 17.

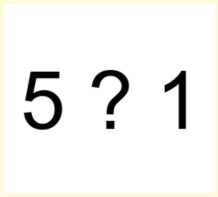

Original Answer: *4*
Detailed Answer: *There are two numbers,* 5 *and* 1*. Performing some mathematical operation gives the answer* 4*. So if we think about adding the numbers,* $5 + 1 = 6$*, subtracting them,* $5 - 1 = 4$*, multiplying them,* $5 \times 1 = 5$*. This implies that the hidden operation must be subtraction (–) and the result is* 4*.*

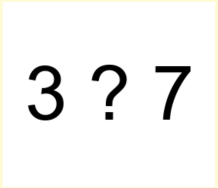

Original Answer: *21*
Detailed Answer: *There are two numbers,* 3 *and* 7*. Performing some mathematical operation gives the answer* 21*. So if we think about multiplying the numbers,* $3 \times 7 = 21$*, adding the numbers,* $3 + 7 = 10$*, subtracting the numbers,* $3 - 7 = -4$*. This implies that the hidden operation must be multiplication or* $\times$ *and the result is* 21*.*

Figure 16: (Operator Induction Math Reasoning) Few examples of our hand-curated data with mathematical reasoning steps.

Judge Prompt - *"You are given a few in-context examples of a mathematical induction problem. The in-context examples each have an image with two numbers and a '?' which is supposed to be some mathematical operation. You are given a solution that gives the answer and the reasoning on how to calculate that answer using some mathematical operation applied on those two numbers in the image. The task is to induce the correct mathematical operation from the given examples, and use that operation to calculate the result of a query image with different numbers.*

After this, you are then given a reference answer written by experts and a candidate response. The candidate response is in format Reasoning: xxx || Answer: xxx . The reasoning part contains reasoning about how the candidate arrived at the solution, and the Answer part contains their final answer. Your task is to judge if the reasoning and the answer of the candidate response are correct or not after considering the in-context examples, query image, question, reference answer, and your own reasoning of the mathematical induction problem.

The rating should be done on a scale of 0–3, where 0 indicates when the response is ambiguous or does not follow the format, 1 is for when both the reasoning and answer are wrong, 2 is for when either only reasoning or answer is correct, 3 is for when both the reasoning and answer are correct.

Be strict in your judgement and do not give a higher rating unless the candidate response contains accurate reasoning and exact answer. Thorougly check each and every part of the candidate response and make sure it does not contain extra irrelevant operations or answers. If it does then give a lower rating accordingly. The candidate response should follow the format and conclude with the correct answer. If it does not, that means their answer is wrong. Also give your rationale before rating. Give the final rating as > Rating: xxx"

Figure 17: (Operator Induction Math Reasoning) Prompts for the Qwen2.5VL-32B-Instruct to evaluate LMM responses on a scale of 0–3. It is given 1 to 4 in-context examples for understanding the mathematical induction task before the LMM (candidate) response for better evaluation.

We also provide a few examples of LMM predictions for task induction (Figure 18) and perception (Figure 19) and mathematical reasoning (Example 1: Figure 20, 21 and Example 2: Figure 22, 23)

Example (Task Induction): Support shot 1

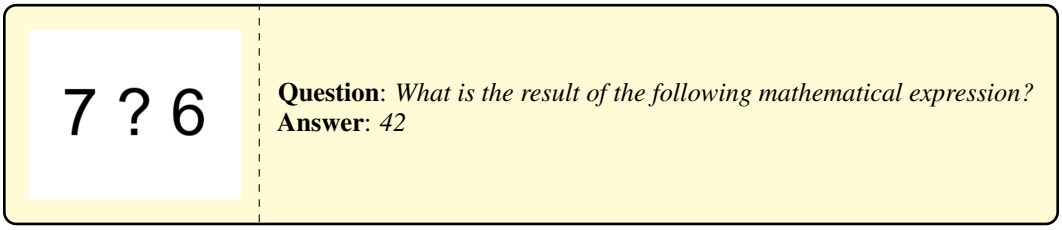

Example (Task Induction): Support shot 2

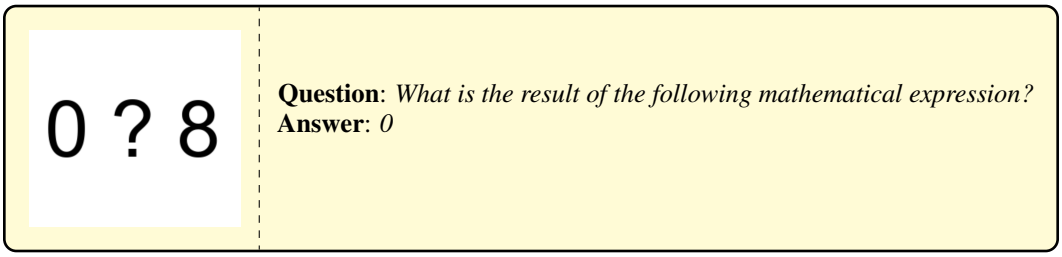

Example (Task Induction): Query

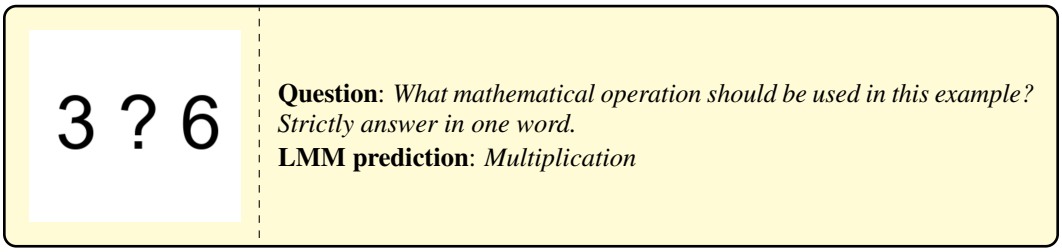

Figure 18: (Operator Induction Task Induction) An example of a 2-shot task induction for multiplication operation

Example (Perception): Support shot 1

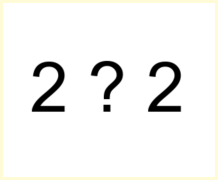

Question: *What is the result of the following mathematical expression?*
Answer: *0*

Example (Perception): Support shot 2

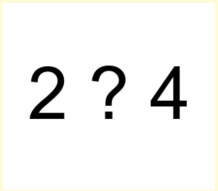

Question: *What is the result of the following mathematical expression?*
Answer: *-2*

Example (Perception): Query

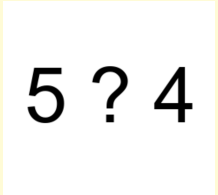

Question: *What are the numbers in this example? Do not calculate the answer after applying mathematical operation. Only give the numbers shown in the example. Stricly give numbers in numeric digits and your result should be in the format > Number A: xxx || Number B: xxx.*
LMM prediction: *Number A: 5 || Number B: 4*

Figure 19: (Operator Induction Perception) An example of a 2-shot perception task to detect operands

Example 1: Support

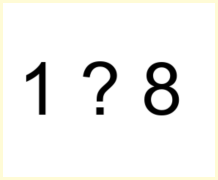

Question: *What is the result of the following mathematical expression?*
Answer: *There are two numbers,* 1 *and* 8*. Performing some mathematical operation gives the answer* 8*. So if we think about subtracting the numbers,* $1 - 8 = -7$*, multiplying the numbers,* $1 \times 8 = 8$*, adding the numbers,* $1 + 8 = 9$*. This implies that the hidden operation must be multiplication or x and the result is* 8*.*

Example1: Query

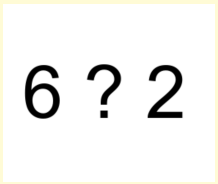

Question: *What is the result of the following mathematical expression? Think step-by-step and give proper reasoning steps first and then given your final answer. The format should be* $>$ *Reasoning: xxx* $||$ *Answer: xxx .The Reasoning part should contain reasons to derive the answer and the Answer part should only contain the answer. Your response should stricly follow this format and not just give the answer of the mathematical operation. It's important that you give reasoning before you answer.*
LMM prediction: *There are two numbers,* 6 *and* 2*. We need to find the result of an operation between them. The question is asking for the result of the operation, which is* 12*. So the answer is Reasoning: The two numbers are* 6 *and* 2*. The operation between them is multiplication.* $6 \times 2 = 12$ $||$ *Answer:* 12

Figure 20: (Operator Induction Math Reasoning) An example of a 1-shot mathematical reasoning task with Judge Rating: 3 (shown in Figure 21)

Example 1: Judge Response

Judge Response – *### Analysis of the Problem*

In-Context Example:
*The in-context example provides the expression '1 ? 8' and states that the result is **8**. The solution explains that among the possible operations (subtraction, multiplication, addition), the operation that yields the result **8** is **multiplication** ('1 × 8 = 8'). This establishes the pattern that the hidden operation is **multiplication**.*

Query Image:
*The query image presents the expression '6 ? 2'. Based on the in-context example, we infer that the hidden operation is **multiplication**.*

Candidate Response:
The candidate response states:
- ***Reasoning**: The two numbers are 6 and 2. The operation between them is multiplication.* $6 \times 2 = 12$.
- ***Answer**: 12*

Reference Answer:
*The reference answer is also **12**.*

Evaluation of the Candidate Response

1. ***Correct Identification of the Operation**: - The candidate correctly identifies the operation as **multiplication** based on the in-context example. This is consistent with the pattern established in the in-context example.*
2. ***Correct Application of the Operation**: - The candidate applies the multiplication operation correctly:* $6 \times 2 = 12$.
3. ***Final Answer**: - The candidate's final answer is **12**, which matches the reference answer.*
4. ***Clarity of Reasoning**: - The reasoning provided is clear and logically follows the pattern established in the in-context example. The candidate explicitly states the operation and shows the calculation step.*
5. ***Format Compliance**: - The candidate response follows the required format: "Reasoning: xxx || Answer: xxx".*

Final Verdict
The candidate's response is both logically sound and mathematically correct. Both the reasoning and the final answer are accurate, and the response adheres to the required format.

*> **Rating: 3****

Figure 21: (Operator Induction Math Reasoning) The Judge (Qwen2.5-VL-32B) evaluates the response of the LMM in Figure 20 to provide correct rating.

Example 2: Support

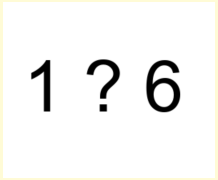

Question: *What is the result of the following mathematical expression?*
Answer: *There are two numbers,* 1 *and* 6*. Performing some mathematical operation gives the answer* 6*. So if we think about subtracting the numbers,* $1 - 6 = -5$*, multiplying the numbers,* $1 \times 6 = 6$*, adding the numbers,* $1 + 6 = 7$*. This implies that the hidden operation must be multiplication or* $\times$ *and the result is* 6

Example 2: Query

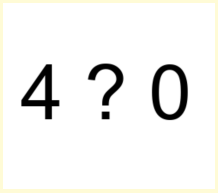

Question: *What is the result of the following mathematical expression? Think step-by-step and give proper reasoning steps first and then given your final answer. The format should be* $>$ *Reasoning: xxx* $||$ *Answer: xxx .The Reasoning part should contain reasons to derive the answer and the Answer part should only contain the answer. Your response should stricly follow this format and not just give the answer of the mathematical operation. Its important that you give reasoning before you answer.*
LMM prediction: *Reasoning: There are two numbers,* 4 *and* 1*. Performing some mathematical operation gives the answer* 5*. So if we think about adding the numbers,* $4 + 1 = 5$*, subtracting the numbers,* $4 - 1 = 3$*, multiplying the numbers,* $4 \times 1 = 4$*. This implies that the hidden operation must be addition or* $+$ *and the result is* 5*.* $||$ *Answer:* 5

Figure 22: (Operator Induction Math Reasoning) An example of a 1-shot mathematical reasoning task with Judge Rating: 1 (shown in Figure 23)

Judge Response – *### Analysis of the Problem*
In-Context Example:
*The in-context example provides the expression '1 ? 6' and the solution states that the result is **6**. The reasoning provided suggests testing different operations:*

- *Subtraction:* $1 - 6 = -5$*;*
- *Multiplication:* $1 \times 6 = 6$*;*
- *Addition:* $1 + 6 = 7$

*From these tests, the solution concludes that the hidden operation is **multiplication**, as* $1 \times 6 = 6$*.*

Query Image:
The query image is '4 ? 0'. We need to determine the result of this expression based on the same hidden operation identified in the in-context example.

Reference Answer:
*The reference answer provided is **0**.*

Candidate Response:
The candidate's reasoning and answer are as follows:
- ***Reasoning**: The candidate incorrectly identifies the numbers as **4 and 1** instead of **4 and 0**. They test different operations:*
- *Addition:* $4 + 1 = 5$*; Subtraction:* $4 - 1 = 3$*; Multiplication:* $4 \times 1 = 4$
- *Conclusion: The hidden operation is **addition**, and the result is **5**.*
- ***Answer**: The candidate concludes that the result is **5**.*

Evaluation of the Candidate Response

1. ***Correct Identification of the Hidden Operation**:*
   - *The in-context example clearly indicates that the hidden operation is **multiplication** (*$1 \times 6 = 6$*).*
   - *However, the candidate incorrectly assumes the hidden operation is **addition** based on their misinterpretation of the numbers.*
2. ***Correct Interpretation of the Numbers**:*
   - *The query image shows the numbers **4 and 0**, but the candidate mistakenly uses **4 and 1** in their reasoning.*
   - *This error leads to incorrect calculations and conclusions.*
3. ***Correct Application of the Operation**:*
   - *Even if we overlook the misidentification of the numbers, the candidate's reasoning is flawed because they do not apply the correct hidden operation (multiplication) as indicated by the in-context example.*
4. *4. **Final Answer**:*
   - *The candidate's final answer is **5**, which is incorrect. The correct answer, based on the reference and the hidden operation of multiplication, should be **0** (*$4 \times 0 = 0$*).*

Rating Justification
*- The candidate's reasoning is **incorrect** because:*

1. *They misidentify the numbers in the query image.*
2. *They incorrectly deduce the hidden operation as addition instead of multiplication.*

*- The candidate's final answer (**5**) is also **wrong**.*

Given these errors, the candidate's response does not align with the in-context example or the reference answer. Both the reasoning and the answer are incorrect.

Final Rating:
> Rating: 1

Figure 23: (Operator Induction Math Reasoning) The Judge (Qwen2.5-VL-32B) evaluates the response of the LMM in Figure 22 to provide correct rating.

A.2.9 SCALING TO MORE SHOTS

Here, we look into the performance of different prompt distillation methods with finetuning-based test time adaptation for larger number of shots and for 3 tasks from the VL-ICL dataset - Operator Induction, CLEVR Count Induction and TextOCR. LMM used for below evaluation is LLaVA-ATT-Qwen2.5 7B (described in Section 3.3). Meta-Tasks used (✓) or not (✗) during training. We see similar performance gains with the introduction of more shots as shown in Table 7. Both the meta-task learning methods, Multi-Task^{PD} and MAPD perform quite well with MAPD showing outstanding performance for Operator Induction.

Table 11: Operator Induction Results.

Training Methods	Meta-task	16-S	32-S	64-S
NoMeta-task^{PD}	✗	73.3	73.3	80.0
Model-Avg^{PD}	✗	71.7	78.3	80.5
In-Context^{PD}	✓	58.3	53.3	76.7
Multi-Task^{PD}	✓	73.3	67.7	80.0
MAPD	✓	**80.0**	**81.0**	**83.3**

Table 12: CLEVR Count Induction Results.

Training Methods	Meta-task	16-S	32-S	64-S
NoMeta-task^{PD}	✗	35.5	30.0	36.5
Model-Avg^{PD}	✗	30.0	34.5	37.0
In-Context^{PD}	✓	25.5	34.5	32.5
Multi-Task^{PD}	✓	38.0	**41.5**	38.5
MAPD	✓	**40.0**	40.5	**41.0**

Table 13: TextOCR Results.

Training Methods	Meta-task	16-S	32-S	64-S
NoMeta-task^{PD}	✗	29.0	26.5	30.5
Model-Avg^{PD}	✗	29.0	29.5	31.5
In-Context^{PD}	✓	26.5	26.0	28.5
Multi-Task^{PD}	✓	27.0	**32.5**	**33.5**
MAPD	✓	**30.5**	31.5	31.5

A.3 Test-Time Compute Analysis for ICL vs FT

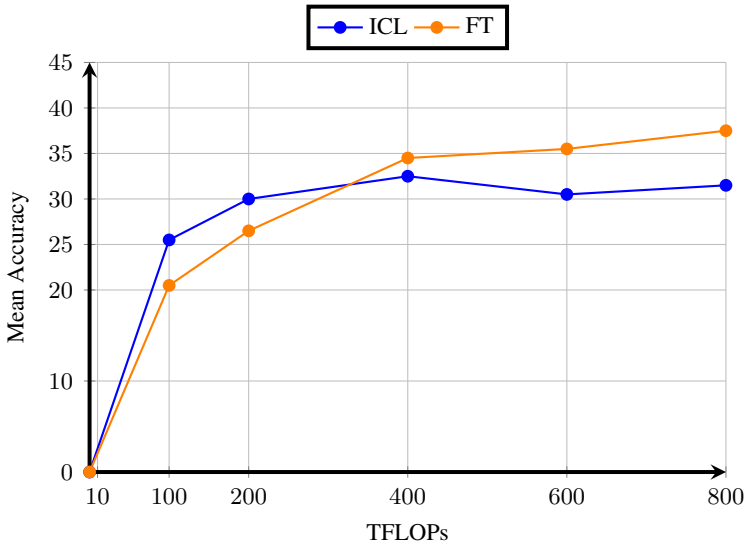

Figure 24: FLOPs matched evaluation on VL-ICL Bench for ICL (blue) vs FT (orange)

We now examine the amount of computation required between different test-time adaptation methods. Figure 24, shows FLOPs-matched evaluation curves for in-context learning (ICL) and fine-tuning (FT), using In-Context^{PD} and MAPD as representative training methods, respectively. We report mean accuracy across all (single-image) VL-ICL datasets. Test-time computation (TFLOPs) scales with the number of shots for ICL, while for FT, it can be scaled by increasing either number of shots or gradient steps. We note that given a low test-time computational budget, ICL performs better than FT, but as the amount of computation is increased FT outperforms ICL. This indicates that FT adaptation is resource-intensive compared to ICL but scales better as the amount of computation is increased at test time.

After 400 TFLOPs, In-Context^{PD} performance begins to decline because the large number of shots used ($\geq$32) exceeds its trained context length of 8,192 tokens. Training In-Context^{PD} with longer context would require $>$4 H200 GPUs, which exceeds our available compute resources. On the other hand, MAPD by design does not require training on long context lengths due to the use of a fixed set of distilled soft prompts for all shots. Additionally, we find that MAPD is much more data-efficient: at 400 TFLOPs, it achieves comparable performance with only 8 shots and 20 gradient steps, indicating better few-shot test-time adaptation.